Roles of TIM-1 in filovirus entry into cells

（フィロウイルスの細胞侵入における **TIM-1** の役割）

Makoto KURODA

CONTENTS

Abbreviations

BDBV	Bundibugyo virus
BiFC	Bimolecular fluorescence complementation
BSA	bovine serum albumin
cDNA	complementary deoxyribonucleic acid
CT	cytoplasmic tail
DAPI	4,6-diamidino-2-phenylindole
DiI	1,1′-dioctadecyl-3,3,3′,3′-tetramethylindocarbocyanine perchlorate
DMEM	Dulbecco's modified Eagle's medium
EBOV	Ebola virus
EIPA	5-(N-ethyl-N-isopropyl) amiloride
FCS	fetal calf serum
FL	fusion loop
GFP	green fluorescent protein
GP	glycoprotein
IB	immunoblotting
IgG	immunoglobulin G
IP	immunoprecipitation
L	RNA-dependent RNA polymerase
LLOV	Lloviu virus
MAb	monoclonal antibody
MARV	Marburg virus
MFI	mean fluorescence intensity

mKG	monomeric Kusabira-Green
MLR	mucin-like region
MLV	murine leukemia virus
MOI	multiplicity of infection
NP	nucleoprotein
NPC1	Niemann-Pick C1
PBS	phosphate buffered saline
Plat-GP	Platinum-GP
pMXs-IG	pMXs-IRES-GFP
PtdSer	phosphatidylserine
RAVV	Ravn virus
RBR	receptor-binding region
RESTV	Reston virus
RNA	ribonucleic acid
SDS	sodium dodecyl sulfate
SDS-PAGE	sodium dodecyl sulfate-polyacrylamide gel electrophoresis
SP	signal peptide
SUDV	Sudan virus
TAFV	Taï forest virus
TAM	Tyro3/Axl/Mer
TIM-1	T cell immunoglobulin and Mucin domain 1
TM	transmembrane domain
VLP	virus-like particle
VP	viral proteins

VSV	vesicular stomatitis virus
WCE	whole cell extract
WT	wild-type

Preface

Viruses in the family *Filoviridae* are filamentous, enveloped, nonsegmented negative-strand RNA viruses that are divided into three genera: *Marburgvirus*, *Ebolavirus*, and *Cuevavirus*. There is one known species of *Marburgvirus*, *Marburg marburgvirus*, consisting of two viruses, Marburg virus (MARV) and Ravn virus (RAVV). In contrast, five distinct species are known in the genus *Ebolavirus*: *Zaire ebolavirus*, *Sudan ebolavirus*, *Taï forest ebolavirus*, *Bundibugyo ebolavirus*, and *Reston ebolavirus*, represented by Ebola virus (EBOV), Sudan virus (SUDV), Taï forest virus (TAFV), Bundibugyo virus (BDBV), and Reston virus (RESTV), respectively[10]. The genus *Cuevavirus* has one species with one known virus named Lloviu virus (LLOV), whose genome sequence was recently detected from dead bats (*Miniopterus schreibersii*) in Spain[57]. Members of the genera *Marburgvirus* and *Ebolavirus* are known to cause severe hemorrhagic fever in humans and nonhuman primates, whereas nothing is known about the pathogenicity of the not yet isolated *Cuevavirus*[42, 57].

In the last decade the frequency of filovirus hemorrhagic fever outbreak increased in central Africa. On March 23, 2014, the World Health Organization reported an outbreak of Ebola virus disease in Guinea, one of the West African countries. Since then the outbreak has spread to seven countries (Sierra Leone, Liberia, Nigeria, Senegal, Mali, Spain, and the United States), resulting in a total of 18,625 confirmed, probable, or suspected cases, including 6971 deaths, as of December 14, 2014, which is far larger than all previous epidemics combined[74]. Although filoviruses pose a significant threat to public health in Western and Central Africa and are of worldwide concern with regard to imported cases and potential bioterrorism, there are currently no approved vaccines or

therapeutics available.

While EBOV-specific immunoglobulin G (IgG) antibodies and viral genomes were detected in serum and two principal organs (liver and spleen), respectively, from three different bat species (*Hypsignathus monstrosus*, *Epomops franqueti*, and *Myonycteris torquata*)[38], MARVs were indeed isolated from healthy cave-dwelling Egyptian fruit bats (*Rousettus aegyptiacus*) in Uganda[4, 75]. Thus, fruit bats have been implicated as potential natural reservoirs of filoviruses, however the transmission route to humans and nonhuman primates remains unclear. On the other hand, other animals have also been reported to be susceptible to filoviruses. RESTV was first isolated from domestic pigs in the Philippines[8] and its genomes were detected in pigs in China[60]. The viral genome was also detected in duikers during EBOV outbreaks in Gabon and the Democratic Republic of the Congo[39]. In addition, serological study have shown that dogs can be susceptible to EBOV infection[2]. These reports suggest that the host range of filoviruses seems to be broader than thus far assumed.

Filovirus particles consist of at least seven structural proteins, including a glycoprotein (GP), a nucleoprotein (NP), viral proteins (VP) 24, VP30, VP35, VP40, and an RNA-dependent RNA polymerase (L) (Figure 1A). The envelope GP is the only viral surface protein and mediates both receptor binding and fusion of the viral envelope with the host cell endosomal membrane during the entry process into cells[72, 81]. Mature GP is composed of two disulfide-linked subunits, GP1 and GP2, which is generated by cleavage of precursor GP by the host protease furin in the Golgi apparatus during virus assembly[79]. GP1 contains a signal peptide (SP), a putative receptor binding region (RBR), and a highly glycosylated mucin-like region (MLR) which shields RBR to protect it from humoral immune responses[37] (Figure 1B and C). GP2 contains a hydrophobic fusion loop

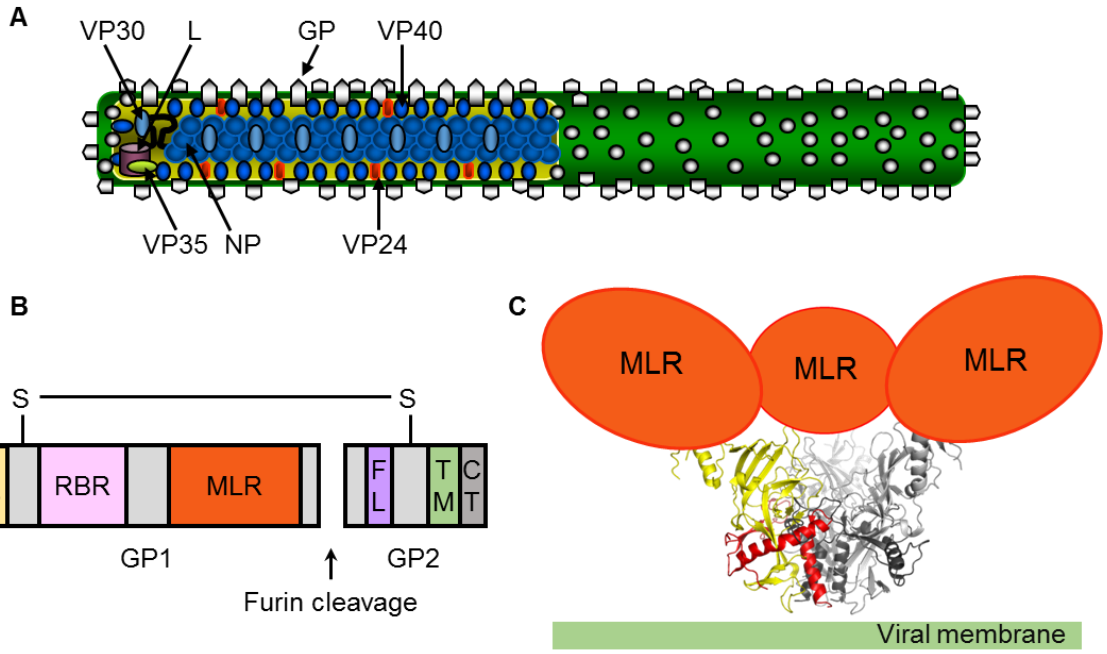

Figure 1. Structure of EBOV particle and envelope GP. Schematic diagrams of EBOV particle (A) and GP are shown (B). (A) GP: glycoprotein, NP: nucleoprotein, VP24: minor matrix protein, VP30: replication-transcription protein, VP35: polymerase cofactor, VP40: major matrix protein, L: RNA-dependent RNA polymerase [70]. (B) SP: signal peptide, RBR; putative receptor-binding region, MLR: mucin-like region, FL: fusion loop, TM: transmembrane domain, CT; cytoplasmic tail. The furin cleavage site is indicated by the arrow. GP1 and GP2 are bound by a disulphide bond. (C) The crystal structure of trimeric EBOV GP (PDB code 3CSY) is prepared by using PyMOL (DeLano Scientific LLC). The predicted position of MLR is shown in orange spheres. A hetero dimer composed of GP1 (yellow) and GP2 (red) is shown.

(FL), a transmembrane domain (TM), and a short cytoplasmic tail (CT) (Figure 1B). On the viral envelope, GP2 exists as a trimer and mediates fusion of viral and host cell membrane[27, 80] (Figure 1C).

During filovirus entry process into cells, GP interact with multiple host molecules (e.g., attachment factors and fusion factor). Infection is initiated by binding of GP to attachment factors, followed by internalization of the virus particle into endosomes via macropinocytosis[1, 56, 64]. In particular, membrane-anchored cellular C-type lectins (e.g., DC-SIGN) interact directly with GP mainly through its MLR that contains a number of N- and O-linked glycosylation sites[3, 9, 20, 41, 43, 44, 71]. T-cell immunoglobulin and Mucin domain 1 (TIM-1) and Tyro3/Axl/Mer (TAM) receptor family facilitates GP-independent virus attachment via direct and indirect binding to phosphatidylserine (PtdSer) on the viral envelope, respectively[28, 48, 52-54]. After internalization, vesicles containing virus particles mature to late endosomes and/or lysosomes, in which low pH leads to proteolytic processing of GPs by cysteine proteases such as cathepsins[12, 50, 66]. Although the initiation of the conformational change in GP leading to membrane fusion is not fully understood, it has been suggested that the proteolytically digested GP exposes the putative RBR, which then interacts with the Niemann-Pick C1 (NPC1) molecule. NPC1 is a large cholesterol transporter protein that localizes in late endosomes and lysosomes[22, 58, 61] and has been shown to serve as a fusion receptor for filovirus entry[11, 14, 49].

TIM-1 was identified as a filovirus receptor candidate using a bioinformatics approach by performing correlation analysis between gene expression profiles of cells and their permissiveness to viral infection[35]. It has been demonstrated that TIM-1 directly interacts with PtdSer on the viral envelope, suggesting that this molecule is important for the GP-independent attachment of viral particles to cells[28, 52, 53]. TIM-1 and related

PtdSer-binding proteins such as TIM-4 and TAM receptor family have subsequently been shown to promote infection of several different enveloped viruses in a manner independent of specific receptor recognition by their envelope glycoproteins[28, 52, 53]. However, TIM-1 contributes in different ways to virus infection. Filoviruses, alphaviruses, flaviviruses, and arenaviruses infection are efficiently enhanced, whereas the infection of other enveloped virus tested such as Lassa virus, herpes simplex virus 1, influenza A virus (H7N1), and SARS coronavirus are not[28, 48, 52].

These cellular attachment factors show distinct expression patterns depending on the tissue or cell type. Filovirus infection of primary target cells such as monocytes, macrophages, dendritic cells, hepatocytes, and endothelial cells[19] is likely dependent on the expression of C-type lectins, whereas infection of other cell types at the late stage of infection[18] seems to rely on multiple attachment factors. However, NPC1 is required for infection and is ubiquitously expressed. Although multiple host molecules are known to be involved in the cellular entry of filoviruses, the molecular mechanisms of filovirus entry which might explain tissue tropism and host range have not been fully understood.

The present thesis consists of two chapters. In the chapter I, I describe a novel role of TIM-1 in filovirus entry into cells and discuss the inhibitory mechanism of filovirus infection by a TIM-1-specific monoclonal antibody (MAb) M224/1. In the chapter II, I show the TIM-1 polymorphism which might be one of the factors influencing cell susceptibility to filoviruses and discuss the role of TIM-1 in filovirus infection.

Chapter I

The Interaction between TIM-1 and NPC1 Is Important for the Cellular Entry of Ebola Virus

Introduction

Filoviruses, including Ebola and Marburg viruses, cause rapidly fatal diseases in humans and nonhuman primates. There are currently no approved vaccines or therapeutics for filovirus diseases. In general, the cellular entry step of viruses is one of the key mechanisms to develop antiviral strategies. However the molecular mechanisms underlying the entry process of filoviruses have not been fully understood.

Filovirus entry is mediated by GP, which is the only surface protein of virions and interacts with multiple host molecules. Among several host molecules proposed as attachment factor[24, 53], TIM-1 is one of the host surface molecules, which has been shown to facilitate PtdSer-mediated virus uptake independently of GP[28, 52, 53]. NPC1 is essential host molecule for filovirus membrane fusion. Proteolytically processed GP, which exposes the putative RBR, interacts with NPC1 and then membrane fusion occurs[11, 14, 49]. While the involvement of several host molecules in each entry step has been revealed, the roles played by their interaction such as initiation of the conformational change in GP leading to membrane fusion remains elusive.

In this chapter, to better understand filovirus cellular entry, I generated MAb M224/1 against TIM-1 molecule that efficiently inhibited filovirus infection of highly susceptible Vero E6 cells and examined its inhibitory mechanism. Interestingly, MAb M224/1 primarily prevented membrane fusion rather than virus attachment. Furthermore, I

demonstrated that the interaction between TIM-1 and NPC1 was important for filovirus entry, suggesting that this interaction could be a novel cellular target for antiviral strategies.

Materials and Methods

Viruses and cells

EBOV (Mayinga strain), SUDV (Boniface strain), TAFV (Taï Forest strain), BDBV (Bundibugyo strain), RESV (Pennsylvania strain), MARV (Angola strain), and vesicular stomatitis virus (VSV) (Indiana serotype) were propagated on Vero E6 cells and stored at -80°C. All infectious work with filoviruses was performed in the biosafety level-4 laboratories at the Integrated Research Facility of the Rocky Mountain Laboratories, Division of Intramural Research, National Institute of Allergy and Infectious Diseases, National Institutes of Health, Hamilton, Montana, USA.

Replication-incompetent pseudotyped VSVs containing the green fluorescent protein (GFP) and luciferase genes instead of the VSV G gene were produced as described previously[55, 72]. Infectivities of VSV bearing filovirus GPs or VSV G were determined by counting the number of Vero E6 cells expressing GFP under a fluorescence microscope or by measuring luciferase activity in infected cell lysates using a Luciferase assay kit (Promega, Madison, Wisconsin, USA).

Human embryonic kidney 293T cells, African green monkey kidney Vero E6 cells, and human leukemic Jurkat T cells from the repository of our laboratory were used for virus infection and host protein expression. 293T-derived Platinum-GP (Plat-GP) cells (Cell Biolabs, San Diego, California, USA) were used for the production of retrovirus vectors. 293T, Plat-GP, and Vero E6 cells were grown in Dulbecco's modified Eagle's medium (DMEM). Jurkat T cells were grown in Roswell Park Memorial Institute 1640 medium. Both media were supplemented with 10% fetal calf serum (FCS) and penicillin-streptomycin.

Generation of M224/1 and virus entry-inhibition assays

Five-week-old female BALB/c mice (Japan SLC, Hamamatsu, Shizuoka, Japan) were immunized via the intraperitoneal route with formalin-fixed Vero E6 cells. Subsequently, splenocytes were fused with B-cell myeloma cells according to standard procedures[68]. Hybridomas were then screened for the ability of secreted MAbs to inhibit the infection of VSV pseudotyped with EBOV GP in Vero E6 cells. MAb M224/1 was obtained screening approximately 1,000 different clones. MAb M224/1 and a control MAb (anti-influenza virus hemagglutinin IgG1, WZ83 59-6-1 from the repository of our laboratory) were purified from mouse ascites using the Affi-Gel Protein A MAPS II Kit (Bio-Rad, Hercules, California, USA). MAb M224/1 was cleaved with papain and its Fab fragments were purified using a protein G separation column (ImmunoPure Fab preparation kit; Thermo Scientific, Waltham, Massachusetts, USA). To evaluate the inhibitory effect of MAb M224/1 on virus infection, Vero E6 cells were pretreated with MAb M224/1 or its Fab fragments for 30 min at 37°C and then infected with filoviruses, VSV, or pseudotyped VSVs at a multiplicity of infection (MOI) of 0.02-0.04 in the presence of the antibody. After incubation for 24-48 hours, cells infected with filoviruses were fixed and stained with a mixture of anti-GP (anti-EBOV 42/3.7 or anti-MARV FS0505)[30, 73] and anti-NP (anti-EBOV 74/7 or anti-MARV FS0609)[13, 29] as primary antibodies and anti-mouse IgG/Alexa Fluor 488 (A11029, Invitrogen Life Technologies, Carlsbad, California, USA) and anti-rabbit IgG/Alexa Fluor 488 (A11034, Invitrogen Life Technologies, Carlsbad, California, USA) as secondary antibodies. Cells infected with VSV were fixed 8 hours postinfection and stained with a mixture of anti-VSV G(N)1-9[55] and anti-VSV M 195-2[44] as primary antibodies, and anti-mouse IgG/Alexa Fluor 488 (A11029, Invitrogen Life Technologies, Carlsbad, California, USA)

as the secondary antibody. Virus infection was quantified measuring the number of fluorescent cells. Filovirus GP-mediated infection was quantified 18 hours post VSV pseudotype inoculation counting the number of GFP-expressing cells under a fluorescence microscope. The relative percentage of infectivity was calculated by setting the number of cells infected in the absence of MAb M224/1 to 100%. Animal studies were carried out in strict accordance with the Guidelines for Proper Conduct of Animal Experiments of the Science Council of Japan. The animal experiments were conducted in strict compliance with animal husbandry and welfare regulations. The mouse study was approved by the Hokkaido University Animal Care and Use Committee (Permit number: 08-0235). The genetic recombination experiments and the microbial experiments were conducted in strict accordance with the Hokkaido University Manual for Safety Management on Genetic Recombination Experiments and the Hokkaido University Biosafety Manual for Handling Pathogens and Other Hazardous Agents, respectively.

Expression cloning

A full-length complementary DNA (cDNA) library was prepared from Vero E6 cells (In-Fusion SMARTer Directional cDNA Library Construction Kit; Clontech Laboratories, Palo Alto, California, USA) and cloned into a murine leukemia virus (MLV)-based retroviral vector, pMX[33]. Plat-GP cells were cotransfected with pMX containing cDNA library genes and a VSV G-expressing plasmid using Lipofectamine 2000 (Invitrogen Life Technologies, Carlsbad, California, USA). Two days later, culture supernatants were collected, and cleared of cell debris by centrifugation at 300 x *g* for 5 min, and by passing through 0.45-μm filters. The clean supernatant was then used for infection of Jurkat T cells at a MOI of 0.15, followed by incubation with MAb M224/1

for 1 hour at 4°C. After washes with cold phosphate buffered saline (PBS), the cells were incubated with anti-mouse IgG/Alexa Fluor 488 (A11029, Invitrogen Life Technologies, Carlsbad, California, USA) and positively stained cells were collected using a MoFlo Astrios cell sorter (Beckman Coulter, Brea, California, USA). The collected cells were propagated until 1 x 10^6 cells were obtained for the next cell sorting. These processes were repeated several times until a cluster of cells expressing the putative target molecule for MAb M224/1 was obtained. Finally, the genomic DNA was extracted from the sorted cell population, and library genes inserted into genomic DNA of the sorted cells were amplified by PCR using library-specific primers and then sequenced.

Generation of TIM-1- and DC-SIGN-expressing cell lines

Coding sequences of Vero E6 TIM-1 (DDBJ accession number AB969733) and human DC-SIGN (GenBank accession number NM021155)[44] were inserted into the MLV retroviral vector pMXs-IRES-GFP (pMXs-IG)[33]. To generate the retrovirus, Plat-GP cells were cotransfected with pMXs-IG encoding Vero E6 TIM-1, its IgV domain-deletion mutant, or DC-SIGN cDNAs and an expression plasmid for VSV G using Lipofectamine 2000 (Invitrogen Life Technologies, Carlsbad, California, USA). Two days later, the retroviruses were collected in the culture supernatants, clarified through 0.45-μm filters, and then used to infect 293T and Jurkat T cells. Transduced GFP-positive cells were collected using a MoFlo Astrios cell sorter (Beckman Coulter, Brea, California, USA) and used for experiments.

Flow cytometric analysis

Parental and transduced 293T cells were detached using 0.25% trypsin, washed with cold PBS/2% FCS, and incubated with MAb M224/1 or the goat anti-TIM-1 polyclonal antibody (AF1750, R&D Systems, Minneapolis, Minnesota, USA). Primary antibody binding was detected with anti-goat IgG/Alexa Fluor 647 (305-606-047, Jackson ImmunoResearch Laboratories, West Grove, Pennsylvania, USA). After several washes, the cells were analyzed employing a FACS Canto flow cytometer (BD Biosciences, Franklin Lakes, New Jersey, USA) and FlowJo software (Tree Star, San Carlos, California, USA). 293T cells cotransfected with the expression plasmids encoding NPC1-monomeric Kusabira-Green (mKG)(N) and/or TIM-1-mKG(C) genes were analyzed using a FACS Canto flow cytometer (BD Biosciences, Franklin Lakes, New Jersey, USA) and FlowJo software (Tree Star, San Carlos, California, USA).

Purification and fluorescence-labeling of Ebola VLPs

Ebola virus-like particles (VLPs) were generated by transfection of 293T cells with the expression plasmids for EBOV VP40, NP, and GP using TransIT LT-1 (Mirus, Madison, Wisconsin, USA). The culture supernatant was harvested 48 hours post-transfection, and cleared of cell debris by centrifugation at 2,000 x *g* for 15 min. VLPs were precipitated through a 30% sucrose cushion by centrifugation at 21,000 x *g* for 1 hour at 4°C using a SW28 rotor (Beckman Coulter, Brea, California, USA). Pelleted VLPs were then resuspended in TNE buffer (10 mM Tris-HCl [pH 7.6], 100 mM NaCl, 1 mM EDTA), and fractionated through a 20-60% sucrose gradient in TNE buffer at 128,000 x *g* for 2.5 hours at 4°C using an SW40 rotor (Beckman Coulter, Brea, California, USA). The membranes of purified VLPs were then labeled with a lipophilic tracer, 1,1′-dioctadecyl-3,3,3′,3′-tetramethylindocarbocyanine perchlorate (DiI) (Invitrogen Life

Technologies, Carlsbad, California, USA), by incubation of the VLPs with a 100 μM solution of DiI in the dark for 1 hour at room temperature with gentle agitation[56].

Real-time imaging of the DiI-labeled VLPs in living cells

Parental Vero E6 cells and Vero E6 cells expressing GFP-Rab7[56] were grown in 35 mm glass-bottom culture dishes (Matsunami Glass, Osaka, Japan). Thirty minutes prior to the experiment the cells were incubated with phenol red-free MEM (Invitrogen Life Technologies, Carlsbad, California, USA)/2% FBS/4% bovine serum albumin (BSA) containing either 50 μg/ml MAb M224/1, 50 μg/ml anti-TIM-1 polyclonal antibody (AF1750, R&D Systems, Minneapolis, Minnesota, USA), 20 mM NH_4Cl, an inhibitor of endosomal acidification, or 100 μM 5-(N-ethyl-N-isopropyl) amiloride (EIPA), a macropinocytosis inhibitor. The cells were then incubated with DiI-labeled VLPs in the same medium in the presence or absence of the antibodies or inhibitors at room temperature for 30 min. The effect of the different temperatures (i.e., 4°C, room temperature, and 37°C) on the VLP attachment has been previously assessed in the same assay and there were no appreciable difference in the total numbers of internalized VLPs across the conditions[56]. Unbound VLPs were removed by washing with medium, and finally the cells were incubated with or without antibodies or inhibitors for various times at 37°C. For the analysis of attachment of DiI-VLPs on the cell surface, cells were fixed in 4% paraformaldehyde for 10 min at room temperature. Nuclei of cells were visualized by Hoechst 33342 staining (Cell Signaling Technology, Danvers, Massachusetts, USA). The cells were analyzed using a Fluoview FV10i confocal laser-scanning microscope (Olympus, Tokyo, Japan). For measurement of adsorbed DiI-VLPs on cell surface, images of 8-10 optical sections were acquired in 1 micron steps. The number of DiI

signals was determined in 50 individual cells (approximately 1-10 dots/cell) and the average number per cell was calculated for each condition. The size and fluorescence intensity of DiI dots were analyzed in 50 individual cells with MetaMorph software (Molecular Devices, Sunnyvale, California, USA).

Immunofluorescence assay

Vero E6 or 293T cells were fixed with 4% paraformaldehyde for 15 min at room temperature and permeabilized with 0.05% Triton X-100 for 15 min. After blocking with 1% BSA in PBS, the cells were stained with the goat anti-TIM-1 polyclonal antibody (AF1750, R&D Systems, Minneapolis, Minnesota, USA), a mouse anti-NPC1 MAb (ab55706, Abcam), or control antibodies, mouse IgG (557273, BD Biosciences, Franklin Lakes, New Jersey, USA) and goat IgG (731635, Beckman Coulter, Brea, California, USA) for 1 hour. Cells were washed 3 times with PBS and first stained with a donkey anti-goat IgG/Alexa Fluor 594 (A11058, Invitrogen Life Technologies, Carlsbad, California, USA). After washing 3 times, cells were then stained with a goat anti-mouse IgG/Alexa Fluor 488 (A11029, Invitrogen Life Technologies, Carlsbad, California, USA) and 4,6-diamidino-2-phenylindole (DAPI) for 1 hour. The cellular localization of TIM-1 and NPC1 was analyzed using an LSM 780 confocal microscope (Carl Zeiss, Oberkochen, Germany) with ZEN 2009 software (Carl Zeiss, Oberkochen, Germany). I confirmed that cross-reactivities of the fluorescent-labeled secondary antibodies to the respective primary antibodies was not appreciably detected and non-specific reaction of the secondary antibodies to cellular components was also minimal (data not shown).

Vero E6 cells and 293T cells transfected with a plasmid expressing TIM-1 were incubated with MAb M224/1 for 30 min on ice and subsequently incubated for 2 hours at

37°C. Cells were fixed with 4% paraformaldehyde for 15 min at room temperature and permeabilized with 0.05% Triton X-100 for 15 min. After blocking with 1% BSA in PBS, the cells were stained with the goat anti-mouse IgG/Alexa Fluor 488 (A11029, Invitrogen Life Technologies, Carlsbad, California, USA) and DAPI for 1 hour. The cellular localization of MAb M224/1 was analyzed using an LSM 780 confocal microscope (Carl Zeiss, Oberkochen, Germany) with ZEN 2009 software (Carl Zeiss, Oberkochen, Germany).

Coimmunoprecipitation assay

The Vero E6-derived TIM-1 gene was C-terminally tagged with FLAG sequence and inserted into a pCAGGS expression vector. The full-length cDNA encoding NPC1 (DDBJ accession number AB971140) was amplified from total RNA extracted from 293T cells by performing RT-PCR with specific primer pairs, C-terminally tagged with HA sequence and cloned into the same expression vector. 293T cells were then transfected with plasmids expressing C-terminally FLAG-tagged TIM-1 (TIM-1-FLAG) and/or C-terminally HA-tagged NPC1 (NPC1-HA) using polyethylenimine. Two days after transfection, cells were washed with PBS and treated with lysis buffer (0.05% NP-40, 20 mM Tris-HCl [pH 7.4], 150 mM NaCl, 10% glycerol) containing protease inhibitors (Halt Protease Inhibitor Cocktail; Thermo Scientific, Waltham, Massachusetts, USA). Cell extracts were mixed with protein G sepharose (GE Healthcare, Little Chalfont, UK) coupled with an anti-FLAG M2 antibody (Sigma-Aldrich, Saint Louis, Missouri, USA) or anti-HA 3F10 antibody (Roche, Basel, Switzerland), and incubated on a rotator at 4°C overnight. The next day, the sepharose beads were washed three times with wash buffer (0.05% NP-40, 20 mM Tris-HCl [pH 7.4], 250 mM NaCl, 10% glycerol), and the

bound proteins were eluted in sodium dodecyl sulfate (SDS) sample buffer, followed by analysis performing sodium dodecyl sulfate-polyacrylamide gel electrophoresis (SDS-PAGE) and immunoblotting with anti-FLAG or HA antibodies.

Bimolecular fluorescence complementation (BiFC) assay

Expression plasmids for TIM-1-mKG(C) and NPC1-mKG(N) were generated by inserting the cDNAs of TIM-1 and NPC1 into fragmented mKG vectors (CoralHue Fluo-chase system; Amalgaam, Nagoya, Japan). 293T cells were cotransfected with the complementary pair of the mKG fusion plasmids. After 24 hours, cells with fluorescent signals derived from complemented mKG molecules accumulated in cells were counted using flow cytometry. The cellular localization of mKG signals was determined using an LSM 780 confocal microscope (Carl Zeiss, Oberkochen, Germany) and ZEN 2009 software (Carl Zeiss, Oberkochen, Germany). Complemented mKG molecules are shown to be little dissociated in cells[21, 76].

Results

Anti-TIM-1 MAb M224/1 blocks filovirus entry into Vero E6 cells

To determine any potential receptor and/or coreceptor molecules required for filovirus entry, I generated mouse MAbs against surface molecules of Vero E6 cells. Assessment of the anti-filoviral activity of the MAbs by studying their ability to block the infectivity of VSV pseudotyped with EBOV GP (VSVΔG-EBOV GP), identified MAb M224/1 (IgG1) as a potent entry inhibitor. Expression cloning using a Vero E6 cDNA library identified TIM-1 as the target molecule of MAb M224/1 (data not shown). TIM-1 consists of two domains, the N-terminal IgV domain that forms a PtdSer-binding pocket and a highly glycosylated mucin domain[45] (Figure 2A). MAb M224/1 recognized full-length TIM-1 on 293T cells but not a mutant lacking its IgV domain (ΔIgV), indicating that the IgV domain is important for the interaction with MAb M224/1 (Figure 2B).

Next, I investigated the ability of MAb M224/1 to inhibit entry and replication of representatives from all known filovirus species (Figure 2C). I observed that replication of all tested filoviruses was dramatically decreased in MAb M224/1-treated cells in a dose-dependent manner. Replication of VSV, which served as a control in this assay, was not substantially affected by MAb M224/1 (Figure 2C), suggesting that this antibody has an inhibitory effect on filovirus infection. Notably, EBOV replication was reduced even when cells were treated with the M224/1 Fab fragment, suggesting that crosslinking by the entire IgG molecule is not required for the inhibitory activity of MAb M224/1 (Figure 2D). Filovirus GP-mediated entry analyzed using VSVΔG-EBOV GP was also considerably inhibited by MAb M224/1 (Figure 2E). Treatment with a control MAb did not show any inhibitory effects even at the highest concentration tested (100 μM) (Figure 2F). These results indicated that this antibody blocked the entry step of filovirus infections

(i.e. attachment, internalization, or membrane fusion).

TIM-1 promotes filovirus infection of human epithelial 293T cells but not of lymphoid Jurkat T cells

Although the effect of TIM-1 on filovirus entry has already been established performing TIM-1-specific siRNA knockdown experiments on Vero cells[35], it remained unclear whether ectopic expression of Vero E6 cell-derived TIM-1 can promote filovirus infection. Therefore, I infected 293T cells, which naturally lack cell surface TIM-1[35], stably expressing Vero E6 TIM-1 with EBOV and VSVΔG-EBOV GP (Figure 3A, left and middle panels), and found that the expression of TIM-1 dramatically enhanced susceptibility of cells to EBOV and EBOV GP-mediated infection, whereas only a limited effect was observed on infection with VSV bearing VSV G protein (VSVΔG-VSV G) (Figure 3A, right panel). These data suggest that EBOV relies on the TIM-1 expression for its efficient cellular entry more substantially than VSV. Interestingly, while expression of DC-SIGN led to productive EBOV and VSVΔG-EBOV GP infection of Jurkat T cells that are poorly permissive for filovirus infections[81], expression of TIM-1 did not (Figure 3B and C). These observations were consistent with previous studies[3, 36], suggesting that there might be a distinct mechanism underlying EBOV GP-mediated entry depending on which attachment factor is used, TIM-1 or DC-SIGN.

M224/1 primarily inhibits viral membrane fusion rather than virus attachment

Since TIM-1 is proposed to serve as an attachment factor for filovirus infection, I first hypothesized that MAb M224/1 inhibits virus adsorption to cells by competing with the PtdSer-binding activity of TIM-1. To analyze this, I generated fluorescent (DiI)-

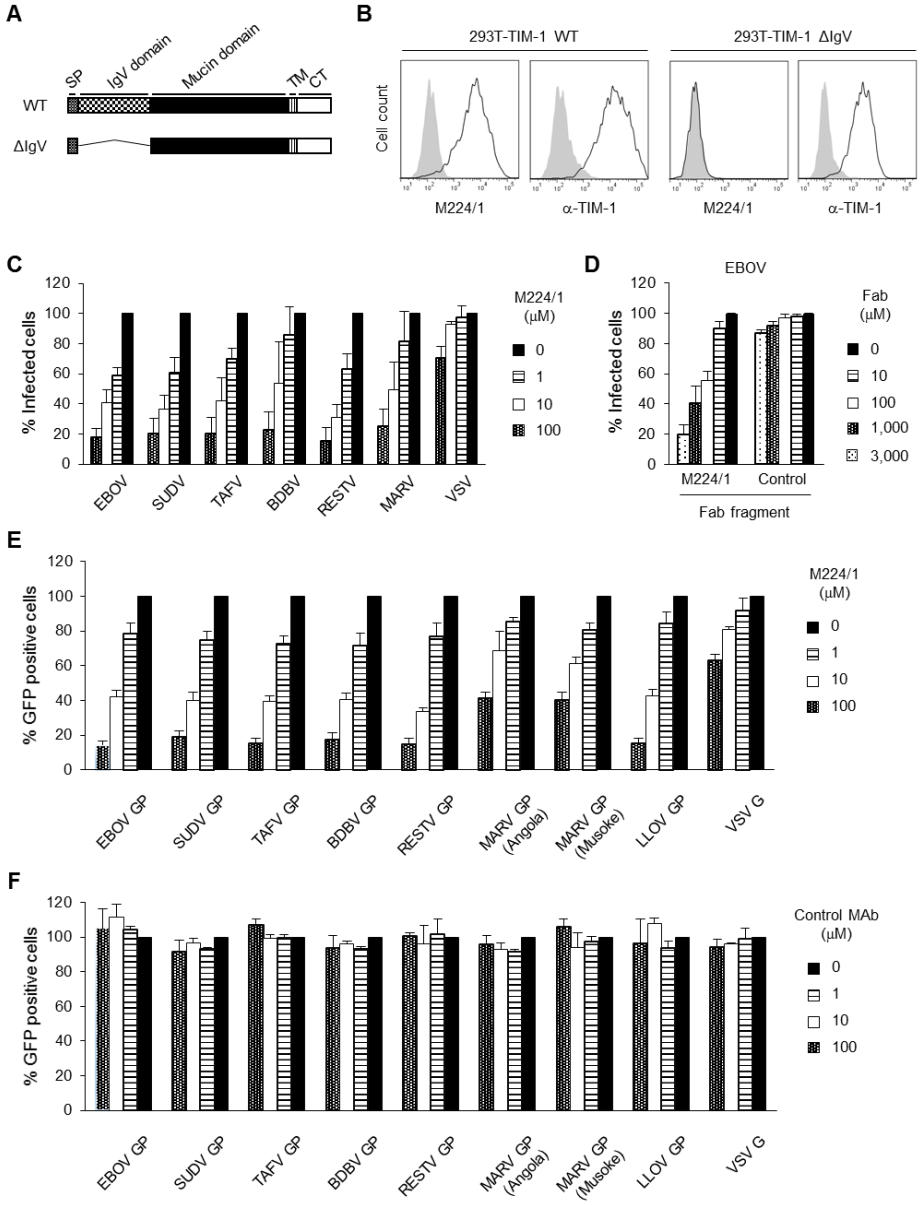

Figure 2. Inhibition of filovirus GP-mediated infection by MAb M224/1 recognizing the IgV domain of TIM-1. (A) Schematic representation of WT TIM-1 and its IgV-deletion mutant (ΔIgV). SP: signal peptide, TM: transmembrane region, CT: cytoplasmic tail. (B) MLV-transduced 293T cells stably expressing Vero E6 TIM-1 WT and ΔIgV were stained with MAb M224/1 or the anti-TIM-1 polyclonal antibody and analyzed by flow cytometry. Black lines represent TIM-1-expressing cells. Gray shadings represent vector-transduced control cells. (C) Vero E6 cells were pretreated with the indicated concentrations of MAb M224/1 for 30 min at 37°C and infected with filoviruses or VSV in the presence of MAb M224/1. Infected cells were stained with virus-specific antibodies and counted. The relative percentage of infected cells was determined by setting the number of untreated infected cells to 100% (approximately 50 to 100

fluorescent cells per microscopic field). (D) Vero E6 cells were infected with EBOV in the presence of M224/1 Fab fragments or a control antibody (WZ83 59-6-1). The relative percentage of EBOV-infected cells was determined as described above. (E,F) In the presence of different MAb M224/1 or control MAb (WZ83 59-6-1) concentrations, Vero E6 cells were infected with VSV pseudotypes bearing the indicated filovirus GP or VSV G. GFP-positive cells were counted and the relative percentage of infected cells was determined as described above. (C-F) The mean of three (C-E) or two (F) independent experiments is shown. Error bars represent standard deviation (SD).

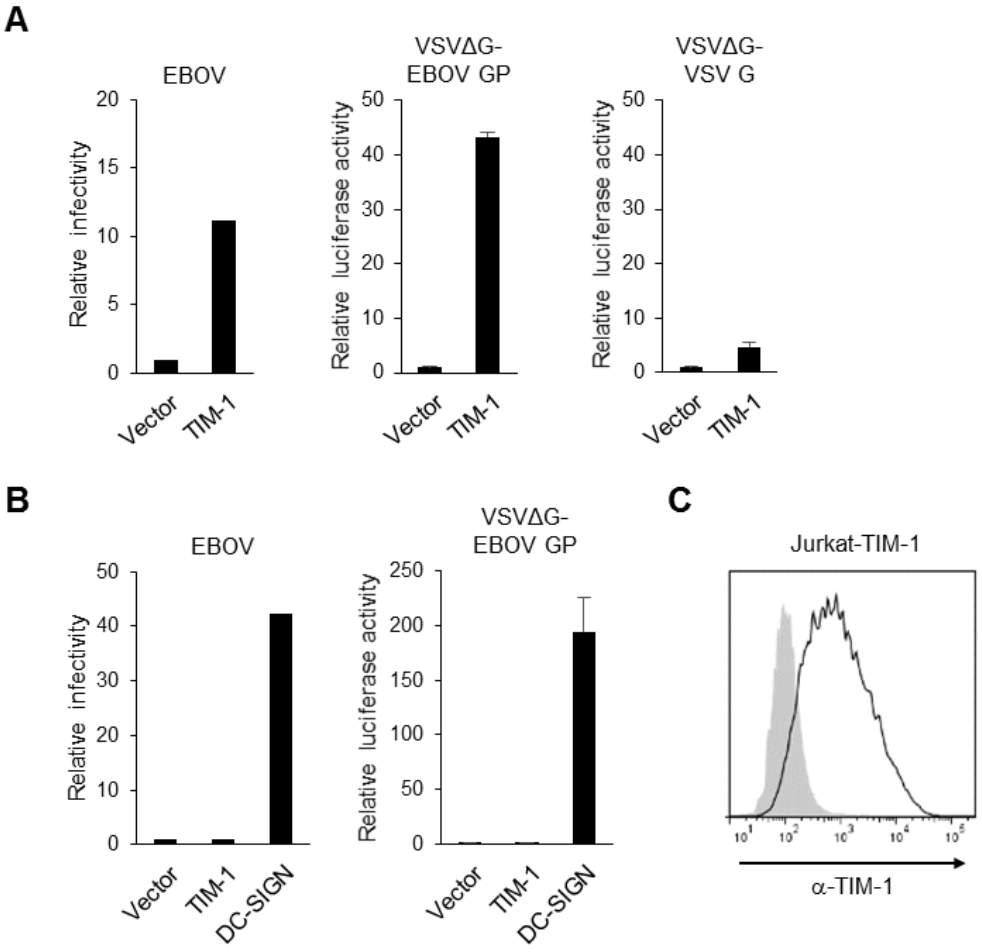

Figure 3. TIM-1-dependent enhancement of infection in 293T cells, but not in Jurkat T cells. (A) 293T cells stably expressing Vero E6-derived TIM-1 and vector-transduced control cells were infected with EBOV (left panel), VSVΔG-EBOV GP (middle panel), or VSVΔG-VSV G (right panel). (B) Jurkat T cells stably expressing Vero E6-derived TIM-1 or DC-SIGN and vector-transduced control cells, were infected with EBOV (left panel), or VSVΔG-EBOV GP (right panel). EBOV supernatant was collected 48 hours postinfection and viral titers were determined by performing 50% tissue-culture-infective dose (TCID50) assay[62]. Luciferase activities of pseudotyped VSVs were measured 24 hours postinfection. The relative infectivity was determined by setting the value (TCID50 or luciferase activity) of infected control cells to 1.0. Each experiment was performed three times. One representative experiment for EBOV is shown. For VSV the mean of three independent experiments is shown. Error bars represent SD. (C) Jurkat T cells stably expressing TIM-1 were stained with anti-TIM-1 polyclonal antibody and analyzed by flow cytometry. Black lines represent TIM-1-expressing cells. Gray shadings represent vector-transduced control cells.

labeled VLPs consisting of EBOV GP, VP40, and NP[40, 59] and compared the number of bound particles on cell surface in the presence and absence of MAb M224/1. Interestingly, I found that the number of VLPs attached to the surface of Vero E6 cells was only slightly decreased in the presence of MAb M224/1, whereas an anti-TIM-1 polyclonal antibody efficiently reduced VLP binding to cells (Figure 4). Consistent with the reduced VLP attachment, a slight reduction of VLP internalization was observed in MAb M224/1-treated cells, whereas many fewer VLPs were detected in cells treated with EIPA, a macropinocytosis inhibitor (Figure 5). Trypsinization of cells after 37°C incubation did not affect the number of visible VLPs (Figure 6), confirming that the internalized VLPs, but not cell surface-bound VLPs, were indeed counted in this assay. The number of VLPs internalized into untreated cells was similar to that measured for cells treated with NH_4Cl, confirming that VLPs detected under assay conditions were likely in a prefusion state. I then analyzed membrane fusion by detection of dequenched DiI fluorescence (Figure 7). In this assay, once the DiI-labeled VLP envelopes fuse with the endosomal membrane, the fluorescent signal is enhanced[23, 56]. In Vero E6 cells expressing GFP-fused Rab7, a late endosome marker, I observed remarkably enlarged and enhanced VLP fusion signals[56] after cells were incubated with DiI-labeled VLPs for 5 hours at 37°C, indicating that membrane fusion occurred in the endosomes (Figure 7A, left panels). In contrast, the DiI signals in MAb M224/1-treated cells were considerably weaker than those in untreated cells and similar to those in NH_4Cl-treated cells (Figure 7A, middle and right panels). Quantification of size and intensity of the DiI fluorescent dots confirmed that their average size and intensity were reduced in MAb M224/1-treated cells compared to untreated cells (Figure 7B and C). I confirmed that the control MAb (WZ83 59-6-1) had no significant effect on the membrane fusion activity (Figure 8). These results suggest

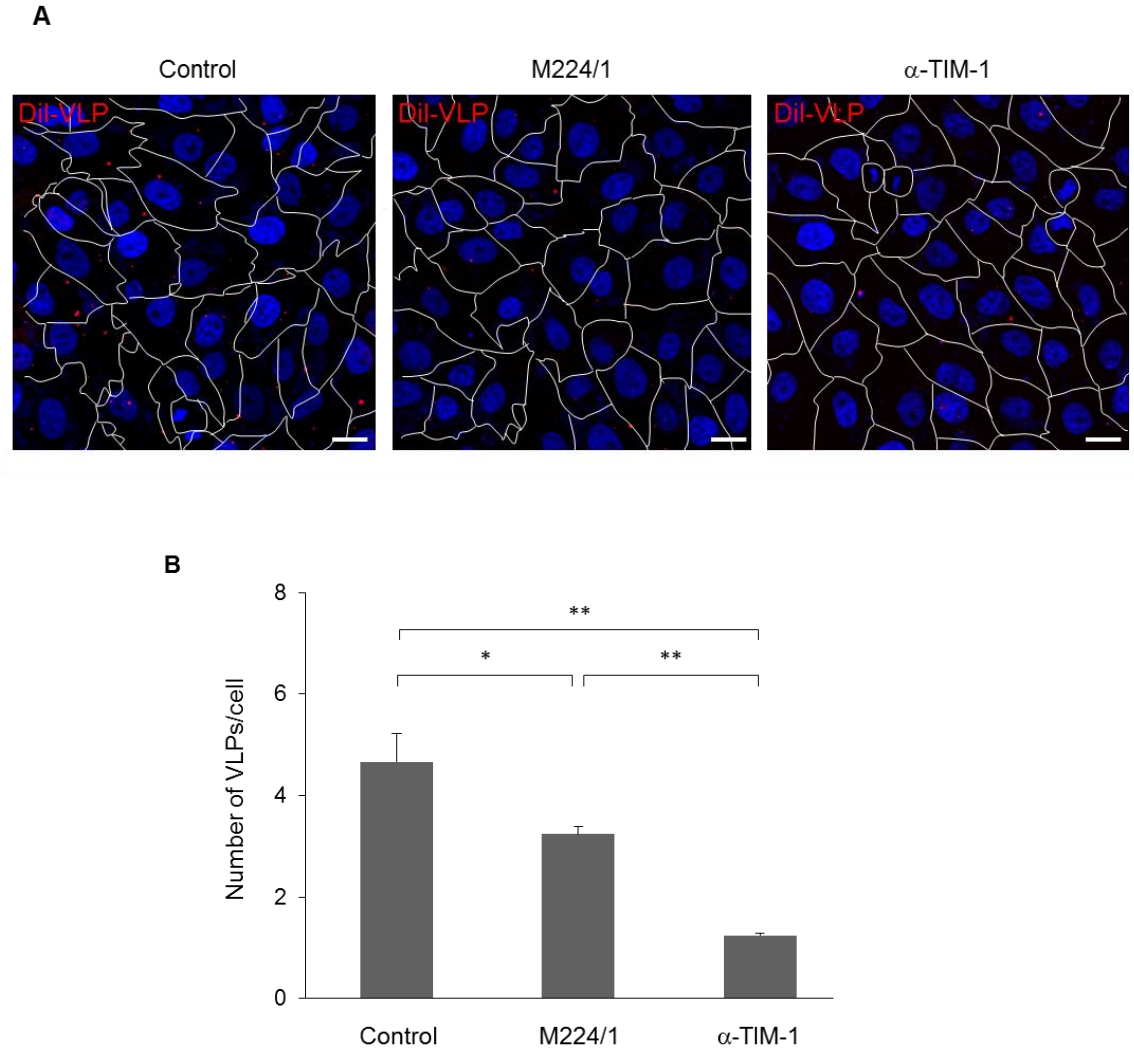

Figure 4. Effects of MAb M224/1 on adsorption of Ebola VLPs to Vero E6 cells. Vero E6 cells were pretreated with or without MAb M224/1 or an anti-TIM-1 polyclonal antibody for 30 min and incubated with DiI-labeled VLPs in the same media, respectively, for 30 min at room temperature. DiI signals (red) were observed using confocal laser scanning microscopy. (A) Images are representative of one experiment performed in triplicate. Nuclei of cells were visualized by Hoechst 33342 staining (blue). Outlines of individual cells were drawn (white). Scale bars represent 20 μm. (B) DiI signals on the cell surface were quantified. The mean of three independent experiments is shown. I confirmed that the control MAb (WZ83 59-6-1) had no significant effect on the membrane fusion activity (see Figure 8). Error bars represent SD. Statistical analysis was performed using student's *t*-test (*$p < 0.05$, **$p < 0.01$).

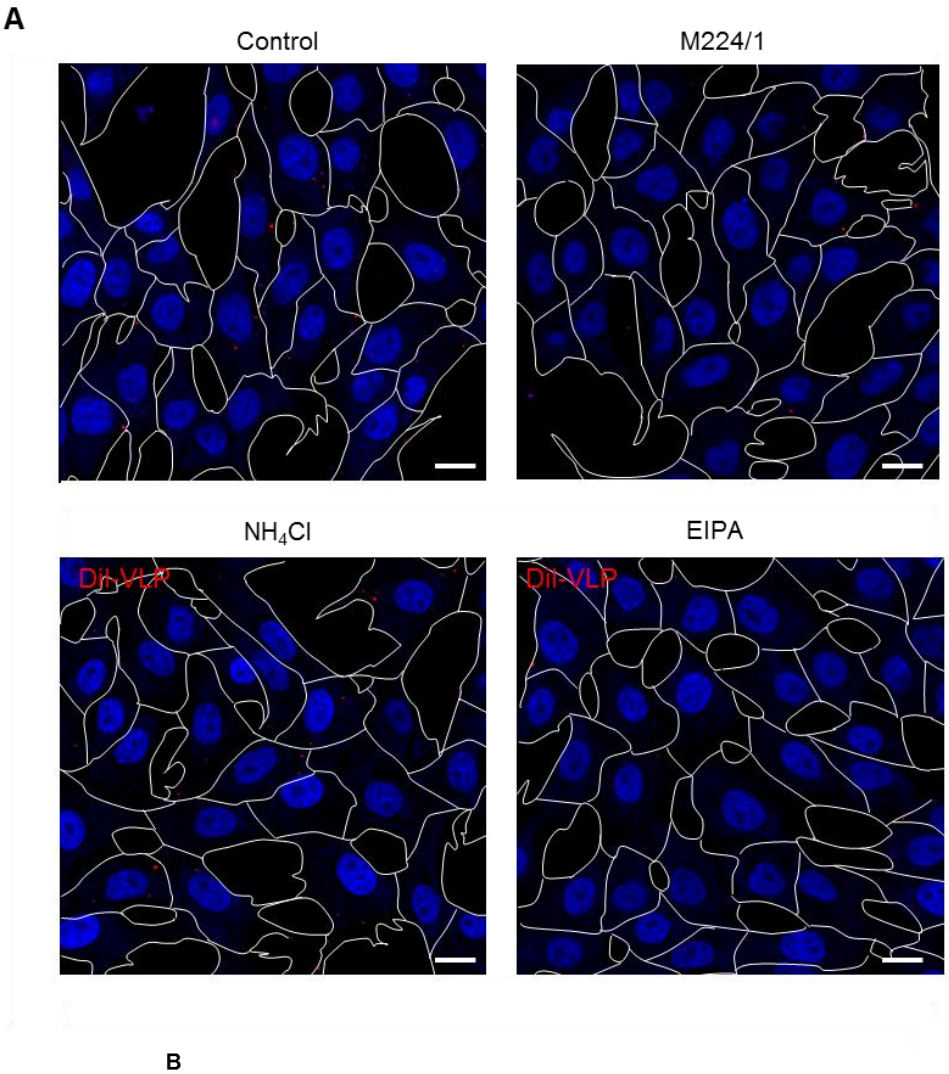
A
Control
M224/1
NH4Cl
EIPA
DiI-VLP
DiI-VLP

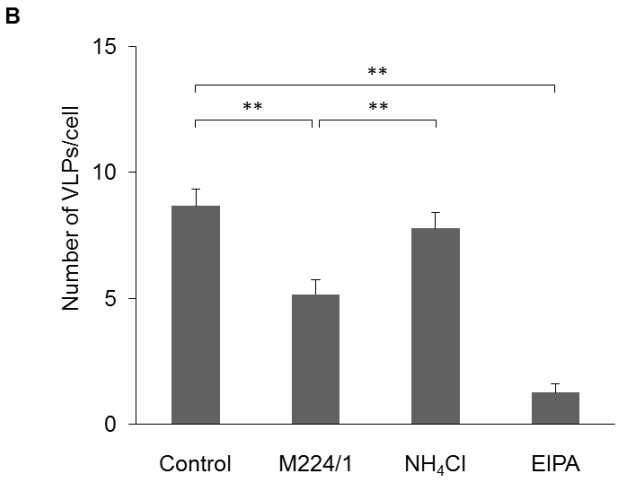
B
Number of VLPs/cell
15
10
5
0
**
**
**
Control
M224/1
NH4Cl
EIPA

Figure 5. Effects of MAb M224/1 on internalization of VLPs into Vero E6 cells. Vero E6 cells were pretreated with or without MAb M224/1, NH_4Cl (inhibitor of endosomal acidification), or EIPA for 30 min and incubated with DiI-labeled VLPs in the same media, respectively, for 30 min at room temperature. After adsorption of DiI-labeled VLPs, cells were incubated for 30 min at 37°C. DiI signals in the cytoplasm at the same focal plane were observed using confocal laser scanning microscopy. (A) Images are representative of one experiment performed in triplicate. Nuclei of cells were visualized by Hoechst 33342 staining (blue). Outlines of individual cells were drawn (white). Scale bars represent 20 μm. (B) DiI signals in the cytoplasm were quantified. The mean of three independent experiments is shown. I confirmed that the control MAb (WZ83 59-6-1) had no significant effect on the membrane fusion activity (see Figure 8). Error bars represent SD. Statistical analysis was performed using student's *t*-test (**$p < 0.01$).

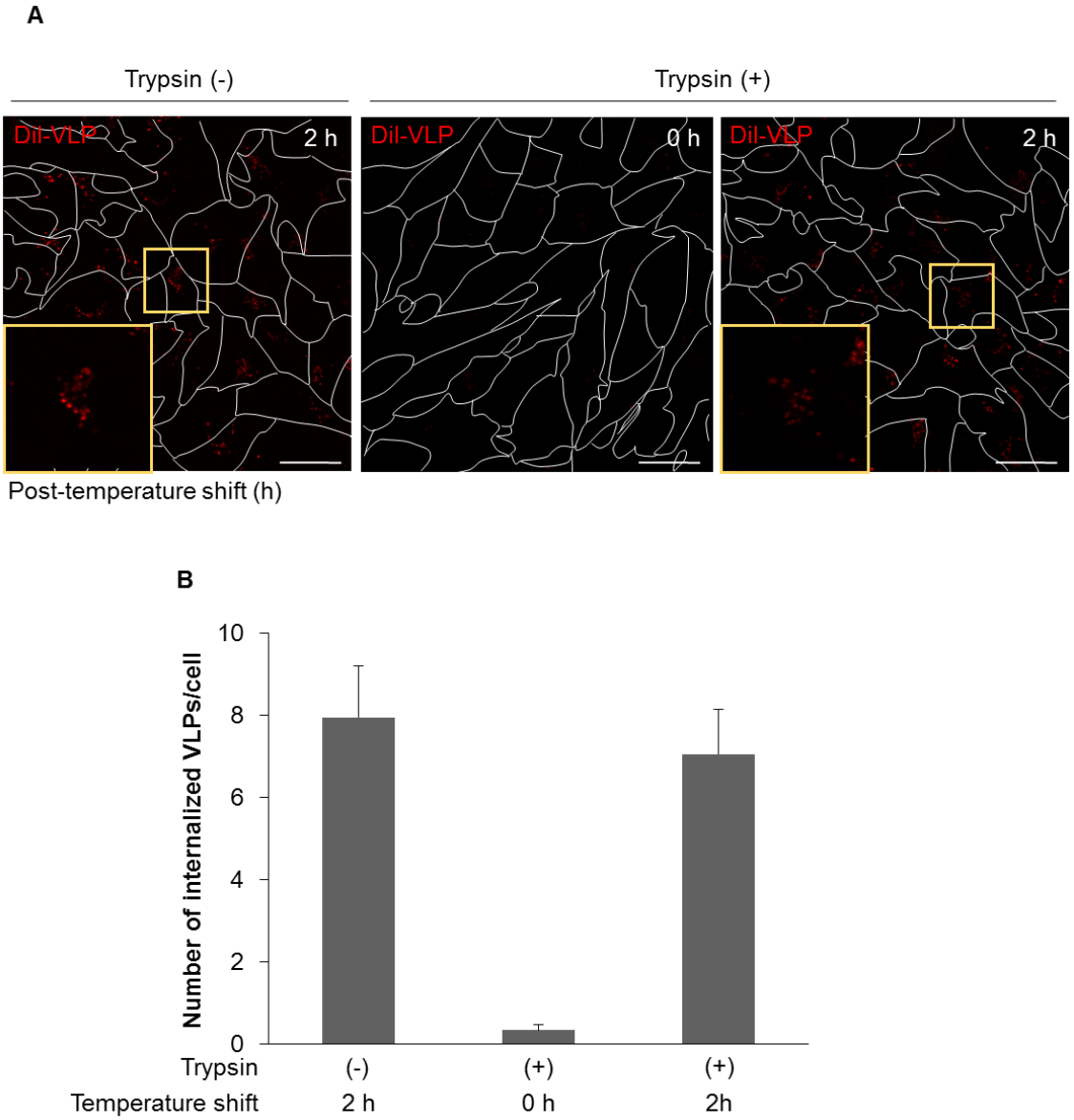

Figure 6. Validation of the number of internalized VLPs. Vero E6 cells were incubated with DiI-labeled VLPs for 30 min at room temperature. After adsorption of DiI-labeled VLPs, cells were incubated at 37°C for 2 hours (A, left panel), treated with 0.25% trypsin for 5 min at 37°C and then incubated at 37°C for 2 hours (A, middle panel), or incubated at 37°C for 2 hours and then treated with 0.25% trypsin for 5 min at 37°C followed by an additional incubation at 37°C for 1 hour (A, right panel). DiI signals in the cytoplasm at the same focal plane were observed using confocal laser scanning microscopy. (A) Images are representative of one experiment performed in triplicate. Outlines of individual cells were drawn (white). Insets show enlargements of the boxed areas. Scale bars represent 20 μm. (B) The internalized DiI-labeled VLPs were measured in 25 individual cells. Each experiment was performed in triplicate. Error bars represent SD.

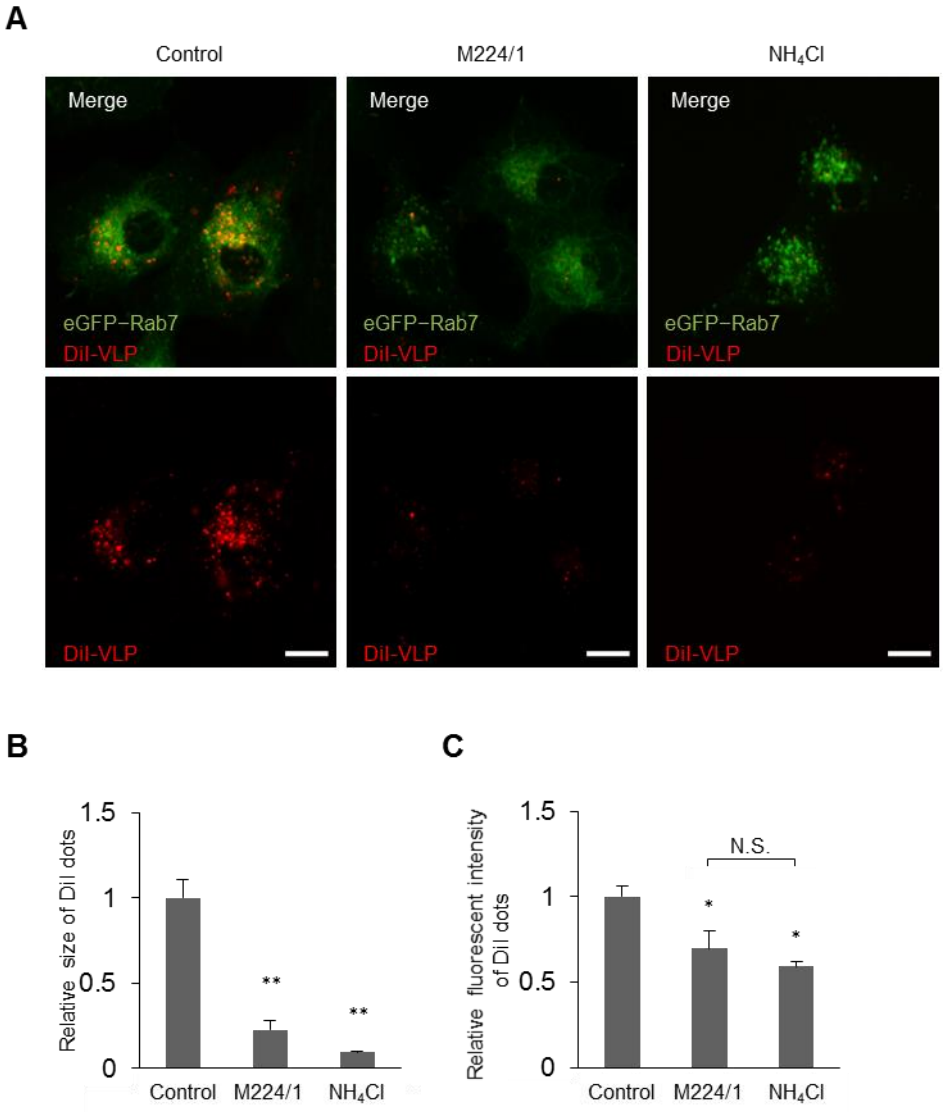

Figure 7. Inhibition of Ebola VLP-induced membrane fusion by MAb M224/1. Vero E6 cells expressing GFP-Rab7 (green) were pretreated with or without MAb M224/1 or NH_4Cl for 30 min and incubated with DiI-labeled Ebola VLPs for 30 min at room temperature. After VLP adsorption, cells were incubated for 5 hours at 37°C in the same media. DiI signals representing VLPs in the cytoplasm were observed in the same focal plane by confocal laser scanning microscopy. Scale bars represent 20 μm. (B,C) Fluorescent intensities of the DiI signals were quantified. Their relative size and intensity of DiI dots were determined by defining the value of untreated infected cells as 1. The mean of three independent experiments is shown. I confirmed that the control MAb (WZ83 59-6-1) had no significant effect on the membrane fusion activity (see Figure 8). Error bars represent SD. Statistical analysis was performed using student's *t*-test (*$p < 0.05$, **$p < 0.01$, N.S.: not significant).

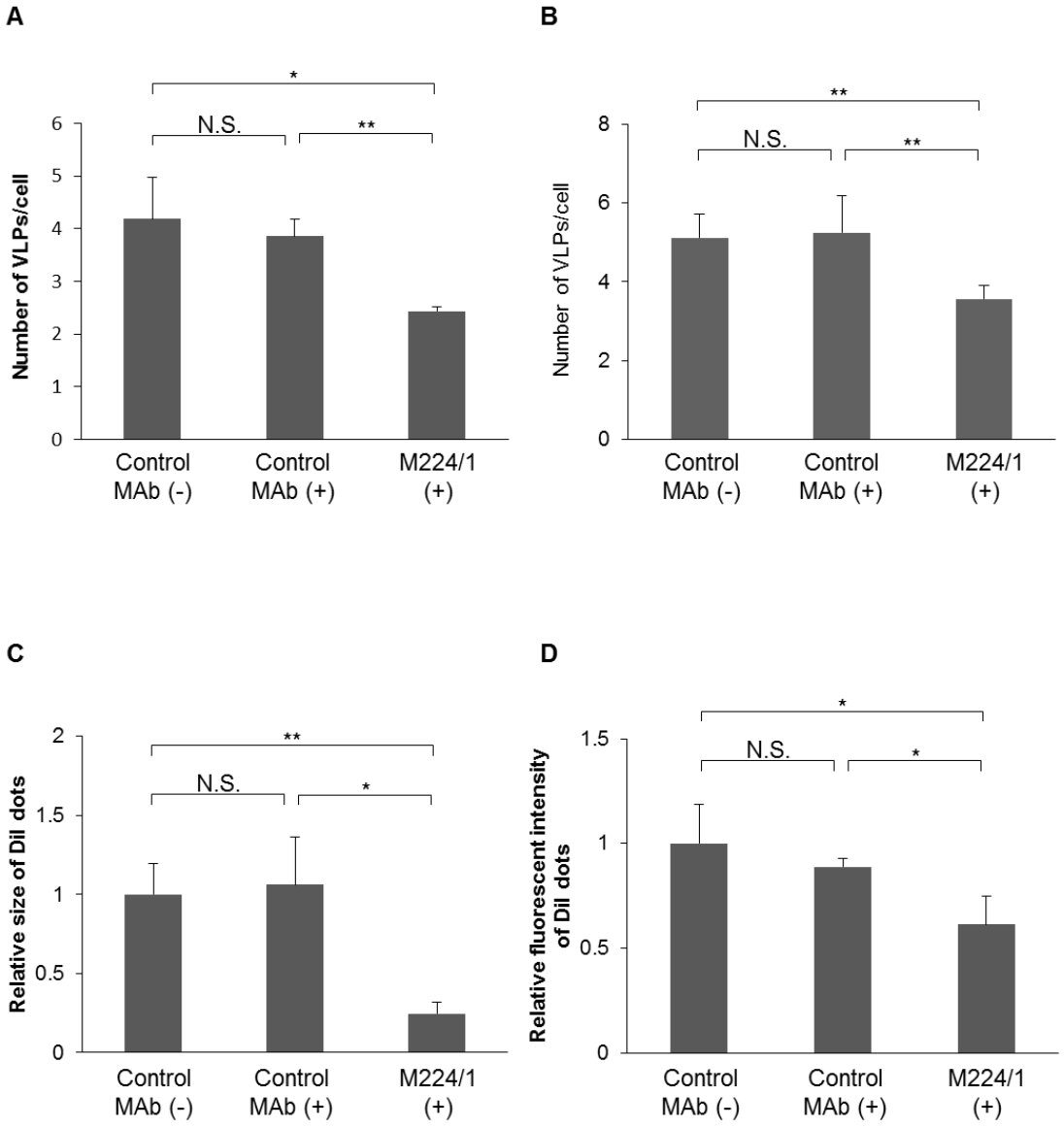

Figure 8. No effect of the control MAb on viral adsorption, internalization, and membrane fusion. Vero E6 cells were pretreated with or without the control MAb (WZ83 59-6-1) or MAb M224/1 for 30 min at 37°C and incubated with DiI-labeled VLPs in the same media for 30 min at room temperature (A). After VLP adsorption, the cells were shifted to 37°C incubation for 30 min (B) or 5 hours (C,D) in the presence of antibodies. DiI signals on the cell surface (A) and in the cytoplasm (B) were quantified by performing confocal laser scanning microscopy. (C,D) Fluorescent intensities of the DiI signals were quantified. Their relative size and intensity of DiI dots were determined by defining the value of untreated infected cells as 1. Each experiment was performed in triplicate. Error bars represent SD. Statistical analysis was performed using student's *t*-test (*$p < 0.05$, **$p < 0.01$, N.S.: not significant).

that MAb M224/1 primarily prevents membrane fusion. Accordingly, I confirmed that cell-bound MAb M224/1 was indeed internalized into intracellular vesicles (Figure 9).

TIM-1 interacts with NPC1

It has been postulated that EBOV membrane fusion occurs in late endosomes and/or lysosomes following the interaction of GP with NPC1, an essential molecule for infection as the fusion receptor[11, 14, 49]. The fact that anti-TIM-1 MAb M224/1 inhibited endosomal membrane fusion led us to hypothesize that TIM-1 might directly interact with NPC1. To confirm this, I first examined the localization of TIM-1 and NPC1 in Vero E6 cells. Consistent with a previous study showing that TIM-1 clusters mostly in the cytoplasm[7], our immunofluorescent assay demonstrated that TIM-1 localized mainly in the cytoplasm (Figure 10A). As previously reported, NPC1 was primarily located in the endosomal and lysosomal membranes in Vero E6 cells. Notably, I found that TIM-1 and NPC1 were mostly colocalized in intracellular vesicles in the cytoplasm (Figure 10A and B). I next examined interaction between TIM-1 and NPC1 by an immunoprecipitation assay (Figure 10C). TIM-1-FLAG and NPC1-HA were expressed in 293T cells and immunoprecipitated using either anti-FLAG or anti-HA antibodies. I found that NPC1-HA was coprecipitated with TIM-1-FLAG captured by the anti-FLAG antibody. Vice versa, TIM-1-FLAG was coprecipitated with NPC1-HA bound by the anti-HA antibody. I further found that while TIM-1 localized in the plasma membrane and perinuclear vesicles in cells transfected with the plasmid, NPC1 was diffusely present in the cytoplasm when expressed alone, but shifted to expression in perinuclear vesicles depending on the presence of TIM-1 (Figure 10B). These results strongly suggested that TIM-1 directly bound to NPC1.

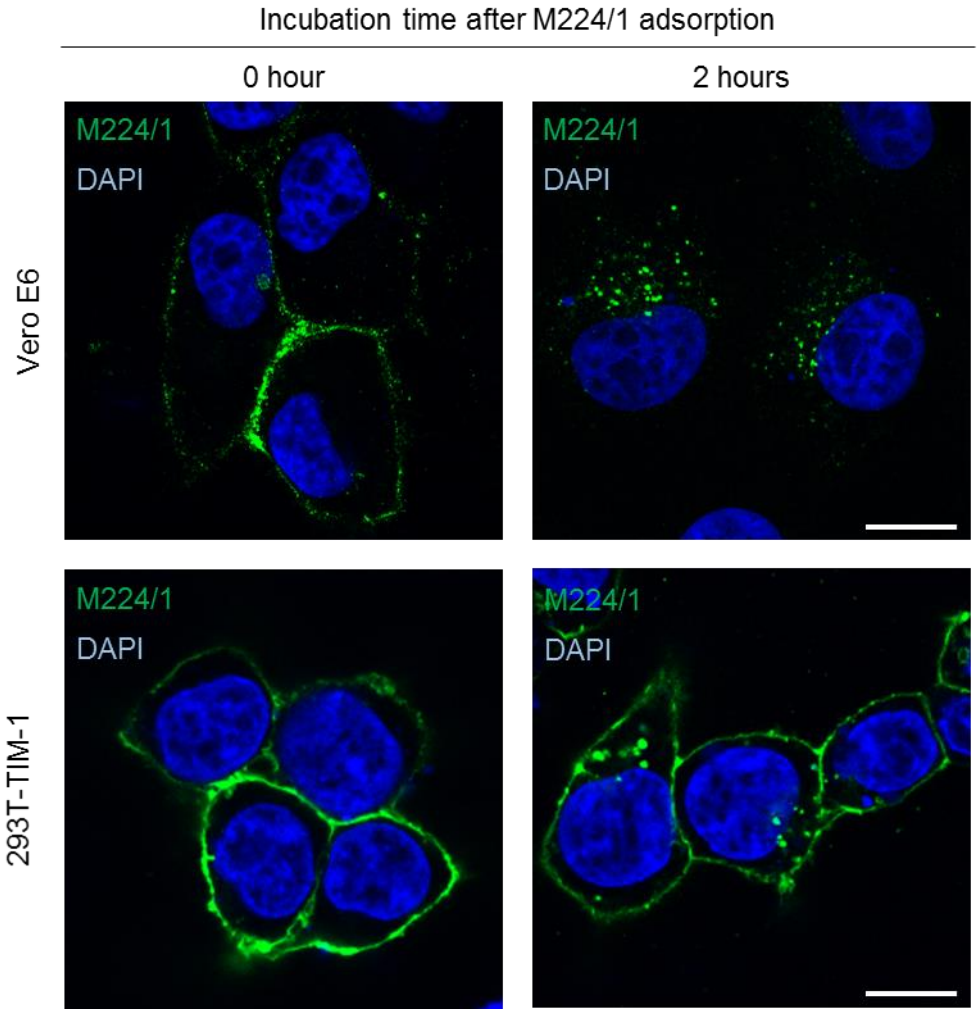

Figure 9. Internalization of TIM-1-bound MAb M224/1 into intracellular vesicles. Vero E6 cells (upper panels) and 293T cells transfected with a plasmid expressing TIM-1 (lower panels) were incubated with MAb M224/1 for 30 min on ice (0 hour) and subsequently incubated for 2 hours at 37°C (2 hours). MAb M224/1 was visualized with anti-mouse IgG/Alexa Fluor 488 and analyzed by confocal laser scanning microscopy. Nuclei of cells were stained with DAPI (blue). Scale bars represent 20 µm.

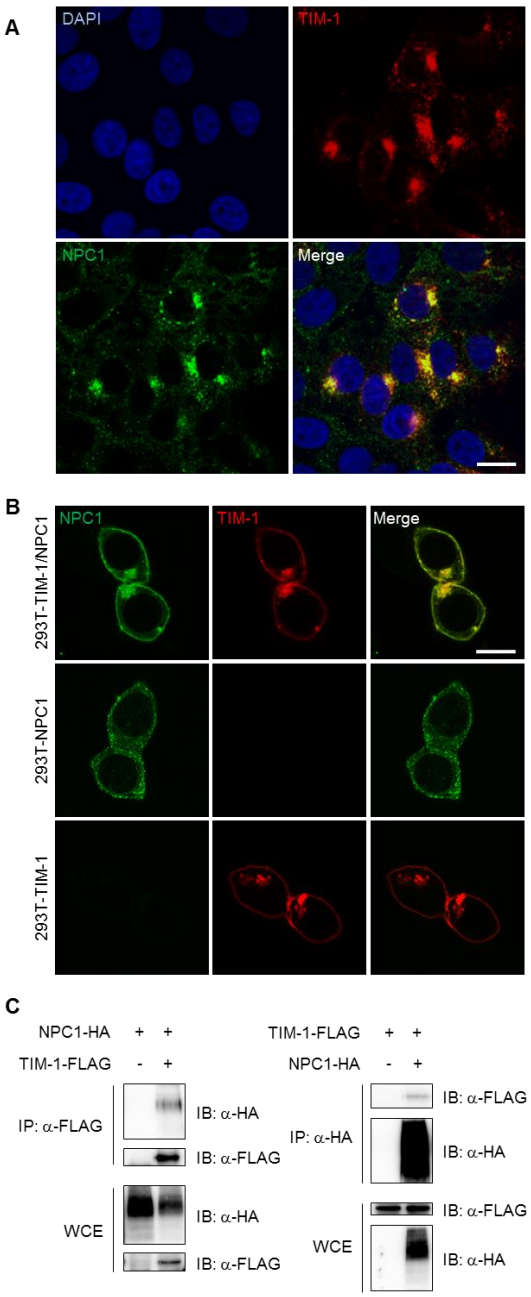

Figure 10. Colocalization and interaction of TIM-1 with NPC1 in Vero E6 cells. (A) Intracellular TIM-1 (red) and NPC1 (green) in Vero E6 cells were visualized with specific antibodies and analyzed by confocal laser scanning microscopy. Nuclei of cells were visualized with DAPI (blue). Scale bars represent 20 μm. (B) Intracellular TIM-1 (red) and NPC1 (green) in 293T cells transfected with plasmids encoding TIM-1-FLAG and/or NPC1-HA were visualized with specific antibodies and analyzed by confocal laser scanning microscopy. Scale bars represent 20 μm. (C) 293T cells were transfected with plasmids encoding TIM-1-FLAG and/or NPC1-HA and subjected to immunoprecipitation (IP) with anti-FLAG (left panel) or anti-HA (right panel) antibodies followed by immunoblotting (IB). WCE: whole cell extract.

M224/1 inhibits the binding of TIM-1 to NPC1

To further characterize the intracellular interaction between TIM-1 and NPC1, a BiFC assay was performed. In this assay, TIM-1 and NPC1 were fused to two inactive fragments of mKG (Figure 11A) and the fluorescence of reconstructed mKG molecules accumulating in cells could be observed only upon complementation of the two molecules. I detected the fluorescence of mKG in 293T cells cotransfected with TIM-1-mKG(C) and NPC1-mKG(N) by flow cytometry, indicating that the binding between TIM-1 and NPC1 occurs intracellularly (Figure 11B). Furthermore, fluorescent microscopy showed that the fluorescence signal was mainly located in intracellular vesicles, not on cell surface (Figure 11C). Next, I investigated the effect of MAb M224/1 on intracellular interaction between TIM-1 and NPC1. I found that the mKG expression was remarkably decreased in MAb M224/1-treated cells and that the number of mKG-positive cells was reduced by the antibody treatment in a dose-dependent manner (Figure 11D and E).

VLP-induced membrane fusion occurs in intracellular vesicles where TIM-1 and NPC1 colocalize and interact

I investigated the colocalization of TIM-1/NPC1 complex with intracellular vesicles (late endosomes/lysosomes) in which VLP-induced membrane fusion occurs. I found that most of the enhanced or enlarged DiI signals representing VLP-induced membrane fusion were associated with mKG-positive cells, and only a limited number of DiI signals were found in mKG-negative cells. This suggested that in cells where the TIM-1/NPC1 interaction takes place (mKG positive), membrane fusion between the VLP envelope and the endosomal membrane could occur more efficiently than in mKG-negative cells (Figure 12A). Higher-magnification images revealed that the enhanced or enlarged DiI

signals (VLPs) colocalized with the mKG signals, the sites of TIM-1/NPC1 interaction in endosomes (Figure 12B). Taken together, these results implied that the interaction between TIM-1 and NPC1 was important for EBOV GP-mediated membrane fusion.

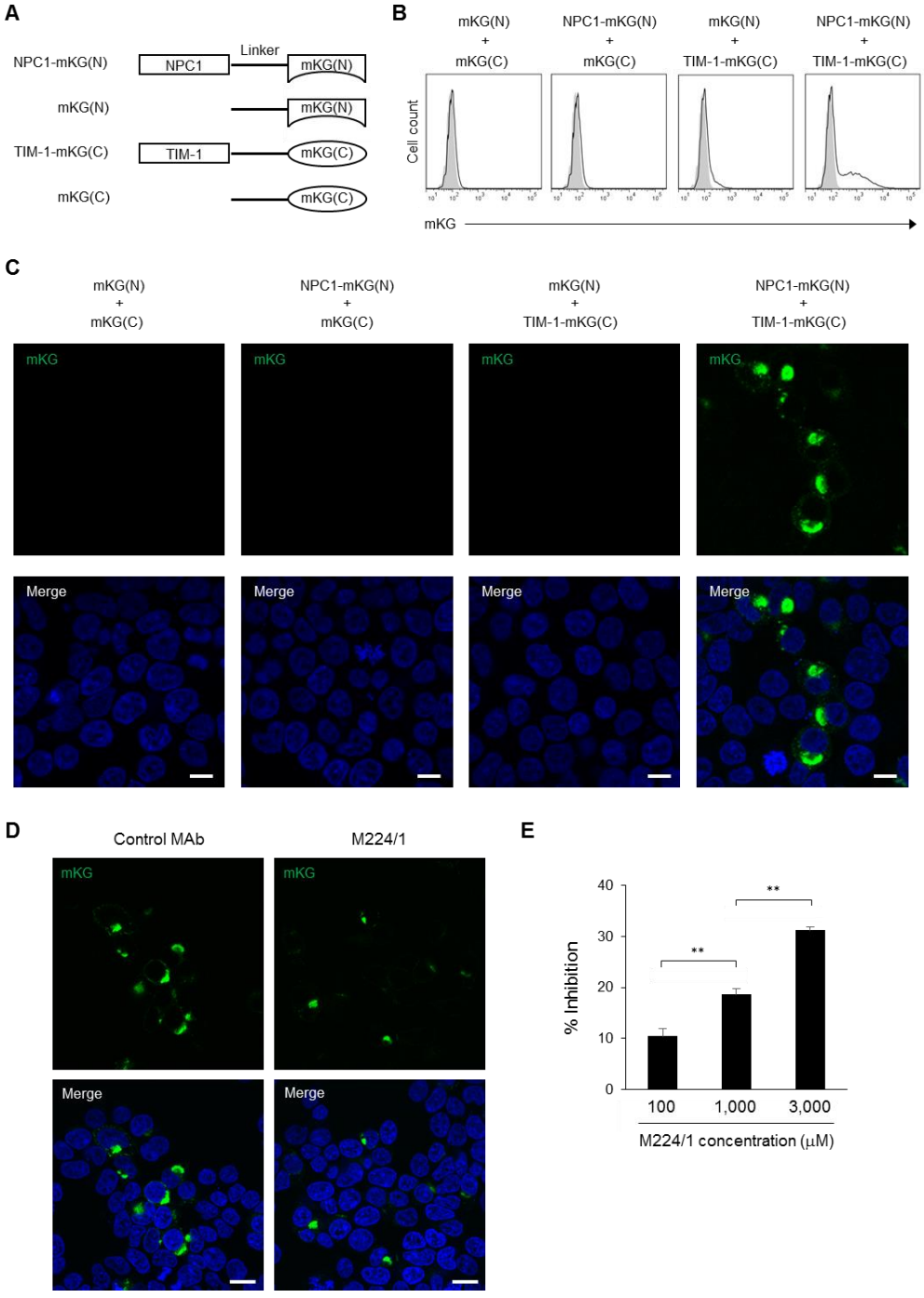

Figure 11. Visualization of the intracellular interaction between TIM-1 and NPC1. (A) Schematic representation of truncated mKG-fused to either TIM-1 or NPC1. mKG(N), N-terminal fragment of mKG. mKG(C), C-terminal fragment of mKG. (B) 293T cells cotransfected with the indicated plasmid pairs were analyzed for mKG signals by flow cytometry 24 hours post-transfection. Opened and closed histograms indicate the cells transfected with the indicated plasmid pairs and the non-transfected cells, respectively. (C) 293T cells were cotransfected with

the indicated plasmid pairs. Cytoplasmic localization of mKG (green) representing the TIM-1/NPC1 binding was visualized by confocal laser scanning microscopy 24 hours post-transfection. Nuclei of cells were stained with DAPI (blue). Scale bars represent 20 µm. (D,E) 293T cells were cotransfected with plasmids encoding NPC1-mKG(N) and TIM-1-mKG(C). (D) At 8 hours post-transfection the cell culture medium was replaced with fresh medium containing 3,000 µM MAb M224/1 or a control antibody. After a 16 hours incubation, mKG signals were detected using confocal laser scanning microscopy. Nuclei of cells were stained with DAPI (blue). Scale bars represent 20 µm. (E) 293T cells were incubated with different concentrations of MAb M224/1 or the control antibody. The number of mKG-positive cells was counted by flow cytometry. The reduced numbers of mKG-positive cells in MAb M224/1-treated cells are presented as percent inhibition compared to the number of mKG-positive cells treated with the control antibody. Each experiment was performed four times and the results are presented as the mean. Error bars represent SD. Significance was calculated using student's *t*-test (**$p < 0.01$).

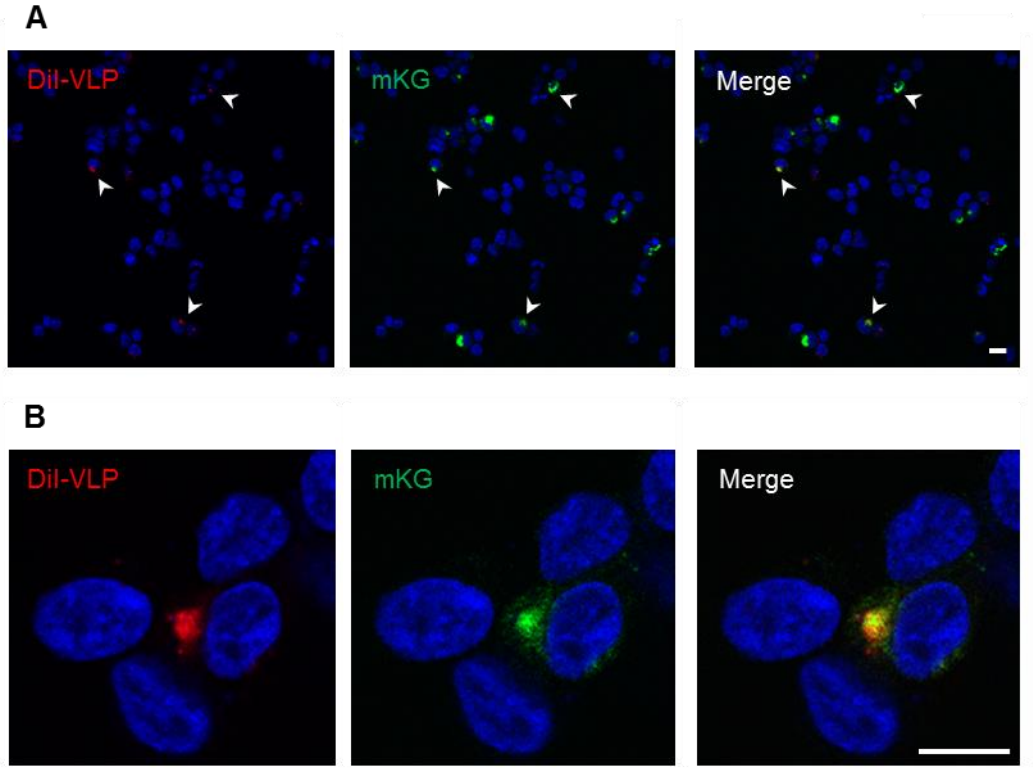

Figure 12. The TIM-1/NPC1 interaction required for EBOV membrane fusion. 293T cells cotransfected with plasmids encoding NPC1-mKG(N) and TIM-1-mKG(C) were incubated with DiI-labeled VLPs for 30 min on ice. The cells were subsequently incubated for 5 hours at 37°C and fixed with 4% paraformaldehyde. DiI (red) and mKG (green) signals in the cytoplasm in the same focal plane were observed using confocal laser scanning microscopy. Nuclei of cells were visualized by Hoechst 33342 staining (blue). Arrowheads indicate the cells in which both mKG (TIM-1/NPC1) and enlarged DiI signals (membrane fusion) were detected. Low (A) and high (B) magnification images are shown. Scale bars represent 20 μm.

Discussion

It is well established that filoviruses utilize multiple host cell molecules for attachment and entry into cells, but the molecular mechanisms underlying this process are not fully understood. While filovirus envelope GPs have been shown to mediate both receptor binding and fusion of the viral envelope with the host cell membrane, a bioinformatics approach previously identified TIM-1 as a GP-independent attachment factor promoting filovirus infection[28, 35, 52, 53]. Using a more classical approach to discover cell surface molecules serving as viral receptors, I also detected TIM-1 and demonstrated its important role in filovirus infection. However, the present study suggests that although TIM-1 promotes filovirus entry, the process is not as simple as just enhanced attachment of the virus particle to cell surface.

Though TIM-1 is mainly expressed on the plasma membrane, intracellular TIM-1 can be detected in early endosomes and lysosomes and has been shown to cycle dynamically to and from the cell surface[7]. Our data also show that TIM-1 is present in intracellular vesicles as well as on the cell surface. Importantly, I found that TIM-1 colocalized and interacted with NPC1 in endosomes where membrane fusion of Ebola VLPs occurred. Although NPC1 has been shown to be essential for GP-mediated membrane fusion in late endosomes/lysosomes during filovirus infection[11, 14, 28, 49], the contribution of intracellular TIM-1 to a post attachment step remained unclear. Our data suggest that TIM-1 is not only involved in filovirus attachment but also in efficient membrane fusion through the interaction with NPC1. It appears that, after internalization of TIM-1-captured virus particles via macropinocytosis, the binding of TIM-1 to NPC1 in late endosomes/lysosomes is required for GP-mediated membrane fusion (Figure 13). This hypothesis is strongly supported by the fact that filovirus infection and EBOV GP-

mediated membrane fusion in Vero E6 cells were considerably decreased in the presence of TIM-1-specific MAb M224/1, which interfered with the binding of TIM-1 to NPC1 in intracellular vesicles (late endosomes/lysosomes).

The proposed model for EBOV entry into cells includes several steps: The first step is GP-dependent (e.g. C-type lectins) or -independent (e.g. TIM-1) virus attachment, which is then followed by the internalization of attached particles via macropinocytosis. Next, GP is cleaved in late endosomes by cysteine proteases such as cathepsins, resulting in the exposure of the receptor-binding region and the final binding of GP to NPC1, triggering membrane fusion. Our results suggest an additional step in this process, the binding of TIM-1 to NPC1, which is important for membrane fusion. I hypothesize that TIM-1 may facilitate the binding of NPC1 to the receptor-binding region in GP by adjacently bridging the endosomal membrane and viral envelope. This event could be important for membrane fusion triggered by the conformational change in GP. Another possibility is that the interaction between TIM-1 and NPC1 directly initiates the conformational change in GP following the binding to NPC1, which then triggers membrane fusion.

However, it is known that filoviruses infect macrophages and dendritic cells, which do not express TIM-1. I hypothesize that previously identified attachment factors such as TAM receptor family (i.e. Tyro3, Axl, and Mer) or yet unknown cellular molecule(s) may have the potential to function as fusion facilitators. Members of the TAM receptor family are expressed on the surfaces of macrophages and dendritic cells[67] and can indeed facilitate PtdSer-mediated virus uptake via indirect binding to PtdSer on the viral envelope[48, 54]. In addition, activated Axl was shown to be internalized by endocytosis and degraded in lysosomes[78]. Therefore, I propose that some other attachment factors may

play a similar role in cells lacking TIM-1.

Under natural physiological conditions, the TIM-1 IgV domain recognizes PtdSer exposed on apoptotic cells and facilitates the clearance of these cells by phagocytosis[25, 34]. PtdSer is also present on the outer membrane of the viral envelope and facilitates virus attachment and uptake via a process known as apoptotic mimicry[28, 52, 53]. Our results demonstrated that the Fab fragment of MAb M224/1 recognizing the IgV domain in TIM-1 inhibited filovirus entry. Taken together our data suggest that MAb M224/1 directly binds to the pivotal site of the IgV domain, which is important for the TIM-1 functions to promote filovirus entry (i.e. PtdSer recognition and interaction with NPC1). Notably, MAb M224/1 significantly prevented membrane fusion (approximately 80%) while its inhibitory effect on virus attachment was limited (30-40%), suggesting that the inhibition of membrane fusion is the principal mechanism of M224/1-mediated reduction of filovirus infections. Therefore, TIM-1 may be primarily involved in the EBOV GP-mediated membrane fusion process rather than virus attachment. I further demonstrated that MAb M224/1 interfered with the binding of TIM-1 to NPC1, suggesting that this novel interaction is likely required for filovirus membrane fusion and may serve as an attractive target for antiviral strategies. Thus, deciphering the detailed structures of the intermolecular interface between MAb M224/1 and TIM-1 or TIM-1 and NPC1 may provide new insights into the development of antivirals such as low-molecular-weight compounds that can be universally used against filovirus infections.

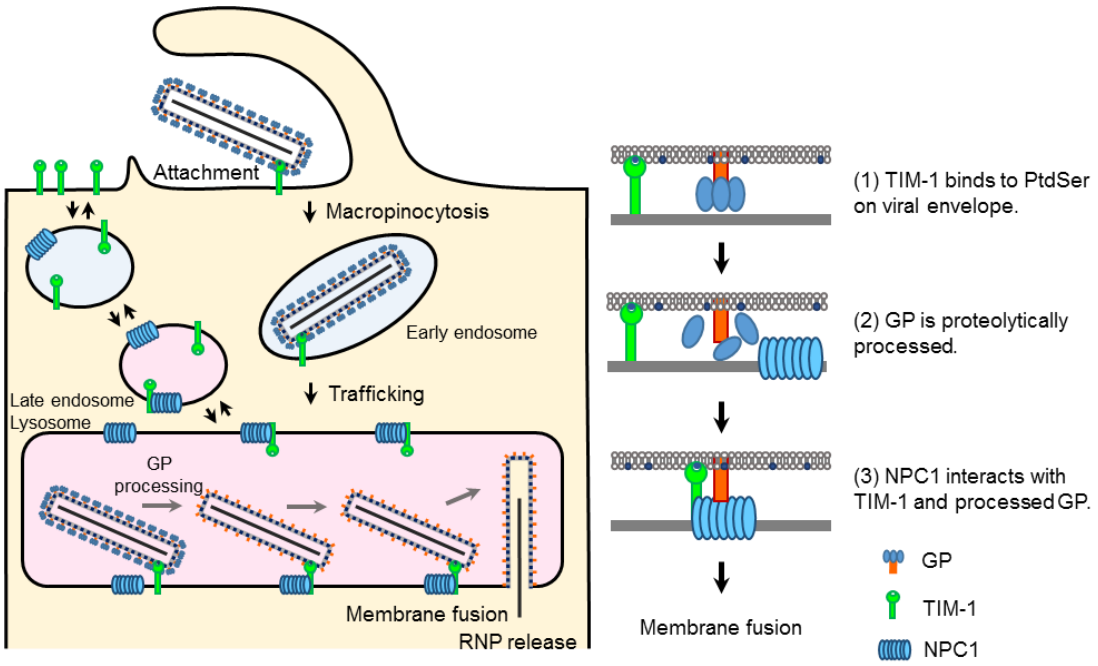

Figure 13. Proposed model of EBOV GP-mediated cellular entry into TIM-1-expressing cells. (1) EBOV attaches to the cell surface via binding of TIM-1 to PtdSer on the viral envelope. (2) After internalization of TIM-1-bound virus particles into early endosomes via macropinocytosis, the virus particles are transported to late endosomes/lysosomes in which the GP is proteolytically processed. (3) NPC1 interacts with TIM-1 and processed GP, leading to membrane fusion and RNP release.

Summary

Multiple host molecules are known to be involved in the cellular entry of filoviruses, including EBOV; TIM-1 and NPC1 have been identified as attachment and fusion receptors, respectively. However, the molecular mechanisms underlying the entry process have not been fully understood. I found that TIM-1 and NPC1 colocalized and interacted in the intracellular vesicles where EBOV GP-mediated membrane fusion occurred. Interestingly, a TIM-1-specific MAb, M224/1, prevented GP-mediated membrane fusion and also interfered with the binding of TIM-1 to NPC1, suggesting that the interaction between TIM-1 and NPC1 is important for the filovirus membrane fusion. Moreover, MAb M224/1 efficiently inhibited the cellular entry of viruses from all known filovirus species. These data suggest a novel mechanism underlying filovirus membrane fusion and provide a potential cellular target for antiviral compounds that can be universally used against filovirus infections.

Chapter II

A Polymorphism of the TIM-1 IgV Domain: Implications for the Susceptibility to Filovirus Infection

Introduction

The envelope GP is the only viral surface protein responsible for both receptor binding (i.e., attachment) and membrane fusion during entry of filoviruses into cells. The expression pattern of receptors/coreceptors is believed to be one of the major factors determining the host range and tissue tropism of filoviruses[70]. While several cellular molecules have been proposed to be filovirus receptors or coreceptors (i.e., attachment or fusion factors), the molecular mechanisms underlying filovirus entry into cells are not fully understood. Human TIM-1 is known to contribute to filovirus entry through the recognition of PtdSer exposed on the virus envelope and facilitates viral attachment and virus uptake independently of GP[28, 35, 52]. The IgV domain, which forms a PtdSer-binding pocket, is thought to recognize PtdSer on viral envelopes and facilitate the binding of virus particles to cell surfaces[28, 52, 53], suggesting that the IgV domain is essential for the TIM-1-mediated enhancement of viral infection.

African green monkey kidney Vero E6 cells are known to be highly susceptible to filovirus infection and are commonly used for filovirus studies. Though a TIM-1 knockdown experiment has demonstrated that Vero cell-derived TIM-1 largely contributes to efficient filovirus entry into cells[35], information on other African green monkey cell lines such as COS-1 and BSC-1, which are also used for analysis of filovirus infection, is limited[72, 81, 82]. In this chapter, I found that Vero E6 TIM-1 had different

primary structures and a greater ability to promote infectivity of VSVs pseudotyped with filovirus GPs than TIM-1s derived from the other cell lines tested. Interestingly, the increased ability of Vero E6 TIM-1 was most likely due to a single amino acid difference at amino acid position 48. These results suggest that a polymorphism of the TIM-1 molecules is one of the factors that influence the cell susceptibility to filovirus infection.

Materials and methods

Viruses and cell lines

Replication-incompetent VSVs containing the GFP and luciferase genes instead of the VSV G protein gene (VSVΔG-VSVG) and VSVs pseudotyped with filovirus GPs were generated as described previously[72]. A neutralizing monoclonal antibody against the VSV G protein, VSV-G(N)1-9[55], was used to abolish the background infectivity of parental VSVΔG-VSVG. Viral infectious units used to calculate the MOI were determined by counting the number of cells expressing GFP. For quantitative comparison of the infectivity in 293T cells and those expressing WT and mutant TIM-1s, the luciferase activity in infected cell lysates was measured using a Luciferase assay kit (Promega, Madison, Wisconsin, USA). The relative luciferase activity was determined by setting the value of infected control (i.e., empty vector-transduced) cells to 1.0. African green monkey kidney cell lines (Vero E6, COS-1, and BSC-1), 293T, and 293T-derived Plat-GP (Cell Biolabs, San Diego, California, USA)[33] were grown in DMEM supplemented with 10% FCS and penicillin-streptomycin.

Cloning of TIM-1 genes

The coding region of the Vero E6 TIM-1 gene was PCR-amplified from a full-length cDNA library prepared from Vero E6 cells (In-Fusion SMARTer Directional cDNA Library Construction Kit; Clontech Laboratories, Palo Alto, California, USA) using primers EcoRI-TIM-1 (5'-CGGAATTCTCAGATACCATCTGGTAGGGTGT-3'), containing an *Eco*RI restriction site, and TIM-1-XhoI (5'-CCCTCGAGACTGACATGTTGGAAGGCCA-3'), containing an *Xho*I restriction site. Coding regions of the COS-1 and BSC-1 TIM-1 genes were PCR-amplified from cDNA

prepared from total RNA extracted from these cells using the same primer pairs. After sequence confirmation (DDBJ accession number AB969733, AB969734, and AB969735 for Vero E6, COS-1, and BSC-1, respectively), these PCR products were cloned into a MLV-based retroviral vector, pMXs-IG[33].

Generation of TIM-1-expressing cells

To generate the retrovirus, Plat-GP cells were cotransfected with pMXs-IG encoding Vero E6, COS-1, or BSC-1 TIM-1 cDNAs and the expression plasmid pCAGGS encoding VSV G cDNA, using Lipofectamine 2000 (Invitrogen Life Technologies, Carlsbad, California, USA)[33]. Two days later, the culture supernatants containing retroviruses were collected, clarified through 0.45-μm filters, and then used to infect 293T cells. Transduced GFP-positive cells were collected using a MoFlo Astrios cell sorter (Beckman Coulter, Brea, California, USA). The percentages of GFP-positive cells in sorted samples were verified as >95% by using flow cytometry.

Flow cytometric analysis

293T cells were detached using 0.25% trypsin, washed with cold PBS/2% FCS, and incubated with a goat anti-TIM-1 polyclonal antibody (AF1750, R&D Systems, Minneapolis, Minnesota, USA). Primary antibody binding was detected with anti-goat IgG/Alexa Fluor 647 (305-606-047, Jackson ImmunoResearch Laboratories, West Grove, Pennsylvania, USA). After several washes, the mean fluorescent intensities (MFIs) of the cells were analyzed using a FACS Canto flow cytometer (BD Biosciences, Franklin Lakes, New Jersey, USA) and FlowJo software (Tree Star, San Carlos, California, USA).

TIM-1 mutagenesis

Mutant TIM-1 genes were generated using a PrimeSTAR Mutagenesis Basal kit (Takara Bio, Shiga, Japan) with primers containing the desired nucleotide substitutions. All mutations were confirmed by DNA sequencing.

Protein structures

A three-dimensional model of TIM-1 IgV structures (Vero E6 and COS1 TIM-1 IgV) were predicted based on the TIM-1 amino acid sequence on mouse TIM-1 (Protein Data Bank code 2OR8) using the protein homology/analogy recognition engine 2 (PHYRE2)[52]. Crystal structures were visualized using JSmol software (http://sourceforge.net/projects/jsmol/).

Results

Expression of TIM-1s in 293T cells and comparison of amino acid sequences among African green monkey kidney cell lines.

TIM-1 genes were cloned from three different African green monkey kidney cell lines (Vero E6, COS-1, and BSC-1) and introduced into 293T cells, which naturally lack cell surface expression of TIM-1[35]. The expression of these TIM-1 proteins on the 293T cell surface was verified by flow cytometry (Figure 14A). Amino acid sequence analyses revealed that Vero E6 TIM-1 had deletions (1 and 23 amino acids) and 6 amino acid substitutions compared with those of COS-1 and BSC-1 cells whose sequences were completely identical (Figure 14B). Thus, I used TIM-1s of Vero E6 and COS-1 in the following experiments to analyze their ability to promote infectivity of VSVs pseudotyped with filovirus GPs.

Difference in the ability to promote entry of VSV pseudotyped with EBOV GP between Vero E6- and COS-1-derived TIM-1s.

To compare the potential to promote filovirus infection between Vero E6 and COS-1 TIM-1s, I prepared 293T cells stably expressing these TIM-1s and examined the infectivity of VSVΔG-EBOV GP (Figure 15A). I found that both Vero E6 and COS-1 TIM-1s enhanced the infectivity of VSVΔG-EBOV GP, and that the virus infected cells expressing Vero E6 TIM-1 more efficiently than those expressing COS-1 TIM-1. The enhancement of the VSVΔG-VSVG infectivity was minimal and no significant difference was found between Vero E6 and COS-1 TIM-1s. Expression levels of TIM-1s on the cell surface were quantified with MFI values obtained by flow cytometry and found to be similar in these cells (Figure 15B and C). These results suggested that Vero E6 TIM-1

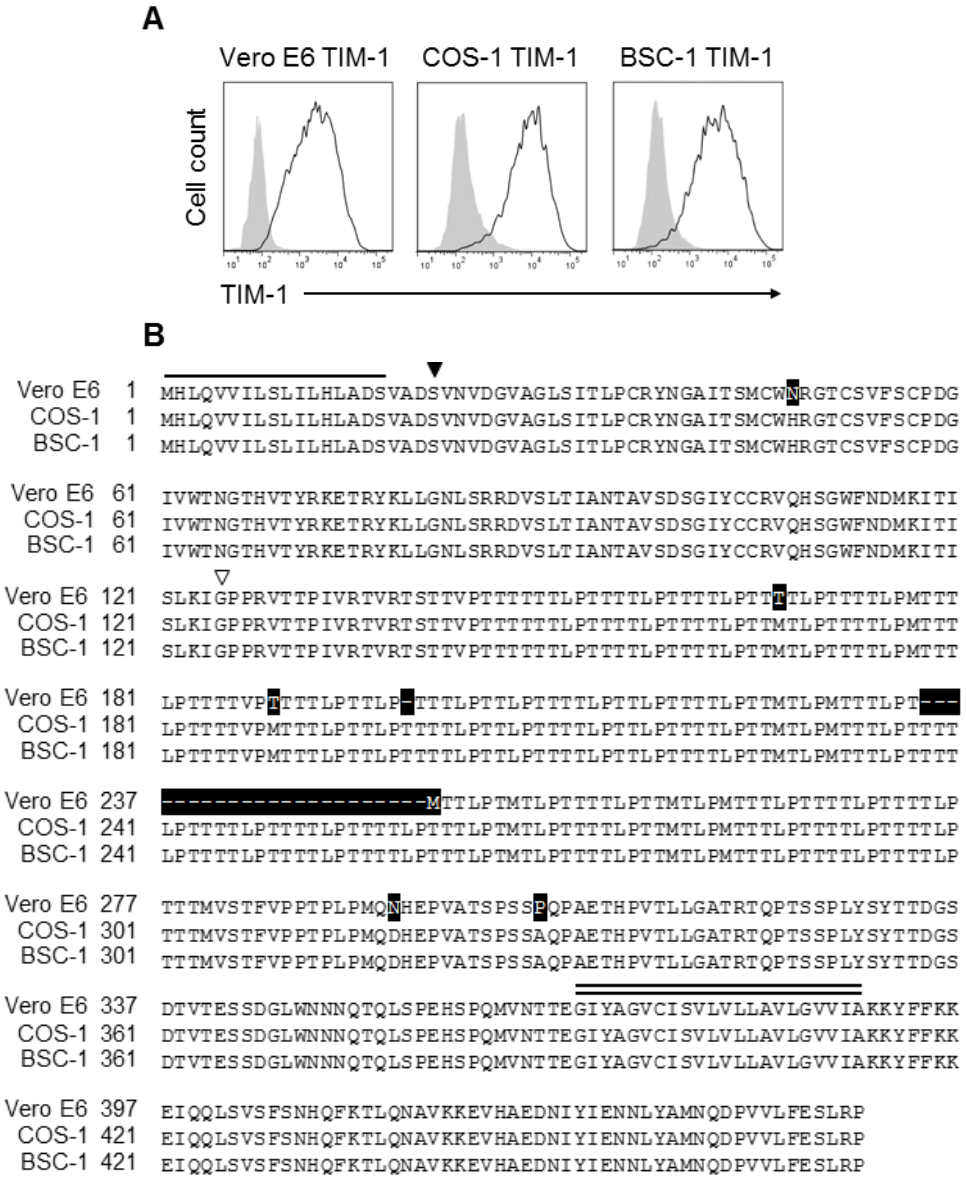

Figure 14. Cloning of TIM-1s derived from three different African green monkey kidney cell lines. (A) 293T cells stably expressing TIM-1s derived from three African green monkey kidney cell lines (Vero E6, COS-1, and BSC-1 cells) were stained with an anti-TIM-1 polyclonal antibody and analyzed by flow cytometry. Open and shaded histograms indicate the fluorescent intensities of the indicated transfectant and vector-transduced control cells, respectively. (B) The deduced amino acid sequences were aligned using GENETYX (version 10). Numbers of residues starting with the respective initiating methionine codons are shown [31]. The signal peptide and transmembrane region are indicated with single and double lines above the Vero E6 TIM-1 sequence, respectively. Black and white arrowheads indicate the beginning of the IgV domain and mucin domain, respectively. Gaps introduced in the sequences for the alignment are indicated by dashes. Black shading indicates non-identical amino acid residues among TIM-1s.

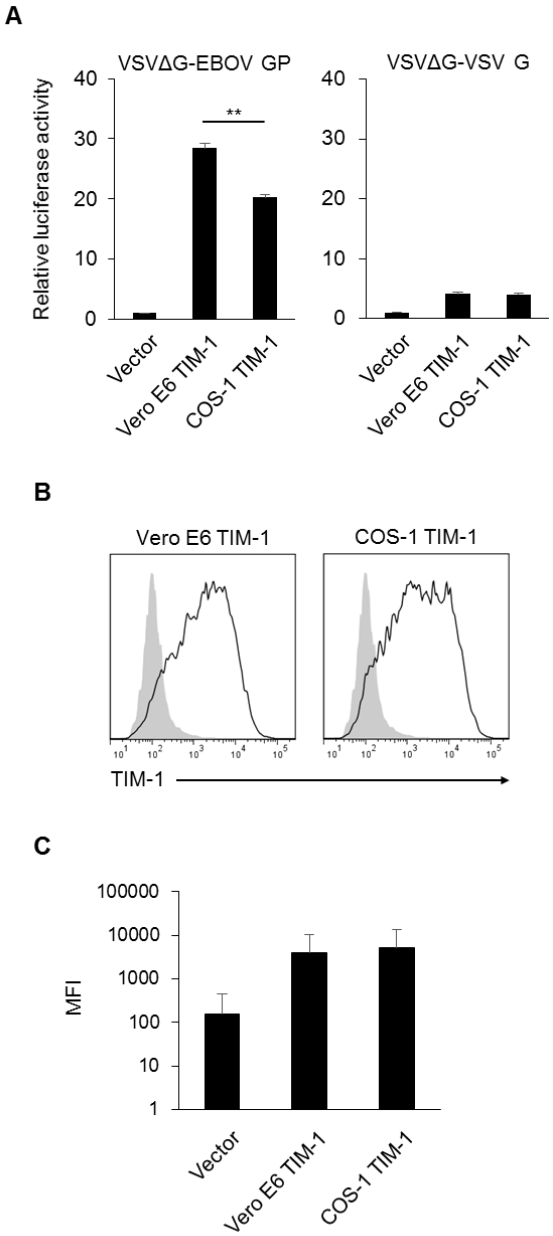

Figure 15. Greater ability of Vero E6-derived TIM-1 to promote entry of VSV pseudotyped with EBOV GP than COS-1-derived TIM-1. (A) 293T cells expressing TIM-1s and control cells were infected with VSVΔG-EBOV GP or VSVΔG-G at a MOI of 0.02-0.04. Luciferase activities were measured 24 hours postinfection. The means of three independent experiments are shown. Error bars represent SD. Significance was calculated using student's *t*-test (**$p < 0.01$). (B,C) 293T cells expressing TIM-1s and control cells were stained with the anti-TIM-1 polyclonal antibody and analyzed by flow cytometry (B) and the TIM-1 expression was quantified using MFI (C). Open and shaded histograms (B) indicate the fluorescent intensities of TIM-1-expressing cells and vector-transduced control cells, respectively.

had greater potential to promote EBOV entry into cells than COS-1 TIM-1.

Importance of the IgV domain for the ability of Vero E6 TIM-1 to promote entry of VSV pseudotyped with EBOV GP.

The IgV domain of TIM-1 is thought to be essential for the TIM-1-mediated enhancement of viral infection[28, 52, 53] and the cytoplasmic tail of TIM-1 is assumed to be involved in intracellular signaling[16, 63, 69]. To clarify whether the IgV domain and/or cytoplasmic tail of Vero E6 TIM-1 were involved in the ability to promote of infectivity of VSVΔG-EBOV GP, I constructed TIM-1-deletion mutants lacking the IgV domain (ΔIgV) or cytoplasmic tail (ΔCT) and examined the viral infectivity in 293T cells expressing these TIM-1 mutants (Figure 16A and B). As expected, with deletion of the IgV domain, TIM-1 completely lost its ability to promote the infectivity of VSVΔG-EBOV GP. Interestingly, ΔCT enhanced the viral infectivity but its efficiency was reduced compared to WT TIM-1. Expression levels of these TIM-1s on the cell surface were quantified with MFI values obtained by flow cytometry and found to be similar (Figure 16C and D). These results indicated that the IgV domain played an essential role in promoting infectivity of VSVΔG-EBOV GP, and that the cytoplasmic tail was also involved in the enhanced infection but not indispensable.

Importance of an amino acid at position 48 in the IgV domain for the increased ability of Vero E6 TIM-1 to promote entry of VSV pseudotyped with EBOV and other filovirus GPs.

Comparison of amino acid sequences of the TIM-1 IgV domain revealed that there was only one amino acid difference, at position 48, between Vero E6 and COS-1 TIM-1s

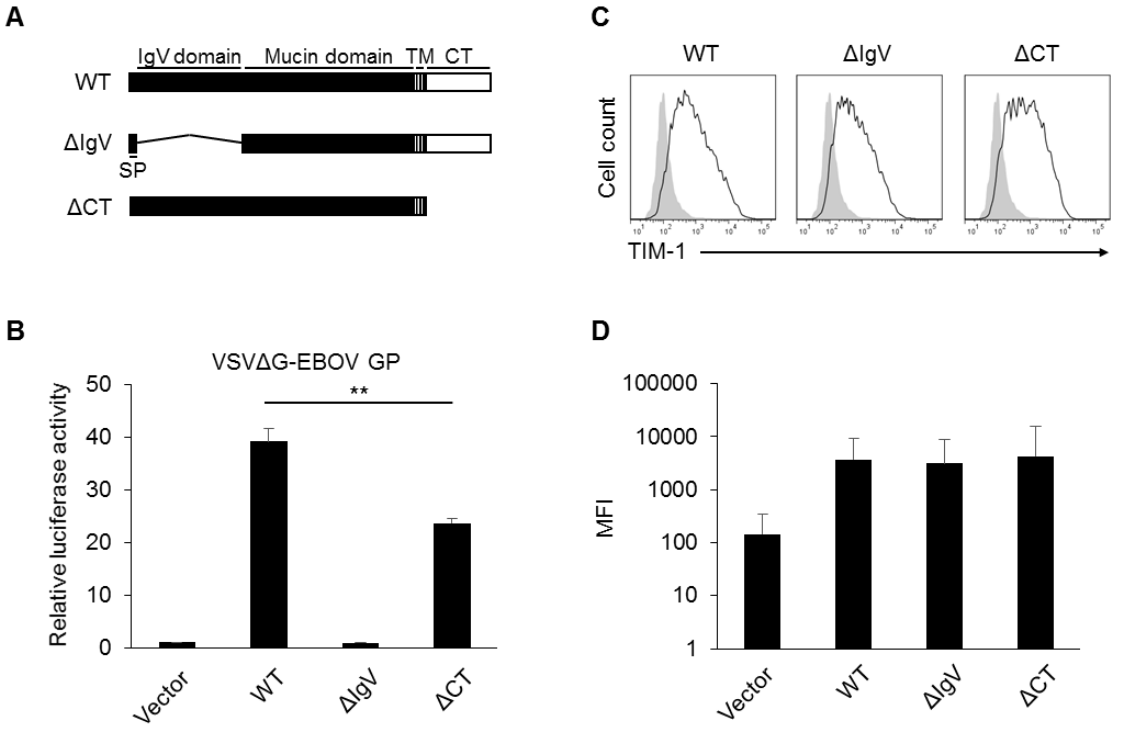

Figure 16. Involvement of the IgV domain and cytoplasmic tail in TIM-1-mediated enhancement of viral infection. (A) Schematic representation of WT and deletion mutant TIM-1s. TIM-1 is a type I transmembrane protein consisting of an N-terminal IgV domain, a highly glycosylated mucin domain, a transmembrane region, and a cytoplasmic tail. SP: signal peptide. TM: transmembrane region. CT: cytoplasmic tail. (B) 293T cells expressing Vero E6 WT, ΔIgV, or ΔCT TIM-1s and control cells were infected with VSVΔG-EBOV GP at a MOI of 0.02-0.04. Luciferase activity was measured 24 hours postinfection. The means and SDs of three independent experiments are shown. Significance was calculated using student's *t*-test (**$p < 0.01$). (C,D) 293T cells expressing Vero E6 WT, ΔIgV, and ΔCT TIM-1s were stained with the anti-TIM-1 polyclonal antibody and analyzed by flow cytometry (C) and the TIM-1 expression was quantified using MFI (D). Open and shaded histograms (C) indicate the fluorescent intensities of TIM-1-expressing cells and vector-transduced control cells, respectively.

(Figure 14B). To confirm that the difference of this amino acid residue affected the potential of TIM-1 to promote efficient filovirus entry, I constructed TIM-1 mutants with single amino acid substitutions in the TIM-1 IgV domain (Figure 17A) and examined the efficacies of these mutants in promoting VSVΔG-EBOV GP infection. Expression levels of these TIM-1s on the cell surface were quantified with MFI values obtained by flow cytometry and found to be similar (Figure 17B and C). I found that N48H (asparagine to histidine) substitution in the Vero E6 TIM-1 IgV domain significantly decreased the virus infectivity (Figure 17D). In contrast, H48N (histidine to asparagine) substitution in the COS-1 TIM-1 IgV domain significantly increased the virus infectivity. These results suggested that the amino acid at position 48 was responsible for cell susceptibility to the increased potential of Vero E6 TIM-1 to promote EBOV entry.

To investigate the potential of TIM-1 to promote infectivities of other filoviruses and the importance of the amino acid at position 48, I prepared VSV pseudotyped with GPs of other filoviruses (RESTV, MARV, RAVV, and LLOV) and examined their infectivities in 293T cells expressing WT and mutant TIM-1s (Figure 17E). Consistent with the result for VSVΔG-EBOV GP, infectivities of VSVs pseudotyped with RESTV, MARV, and RAVV, and LLOV GPs (VSVΔG-RESTV, -MARV, -RAVV, and -LLOV GPs, respectively) were significantly enhanced in 293T cells expressing TIM-1s and the distinct ability due to the single amino acid substitution was commonly observed between WT and mutant TIM-1s. It was noted that the extent of enhancement by TIM-1 expression was much lower for VSVΔG-MARV and -RAVV GPs than for the other viruses tested.

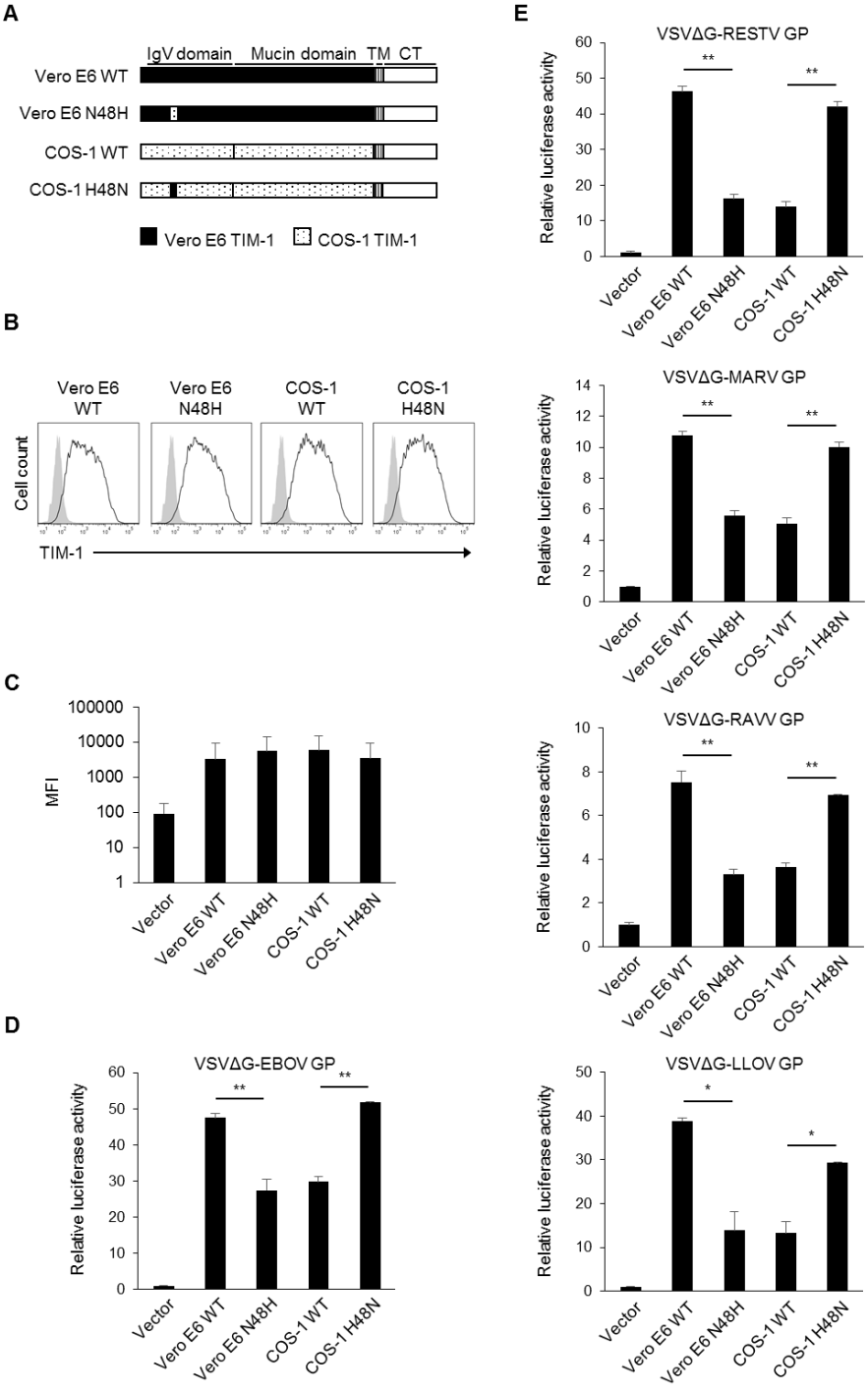

Figure 17. A single amino acid in the TIM-1 IgV domain responsible for the increased ability of Vero E6 TIM-1 to promote entry of VSV pseudotyped with filovirus GPs. (A) Schematic representation of WT and mutant TIM-1s of Vero E6 and COS-1. A Vero E6 mutant TIM-1 containing an asparagine-to-histidine substitution (N48H) and a COS-1 mutant containing a histidine-to-asparagine substitution (H48N) were constructed. (B,C) 293T cells expressing WT

and mutant TIM-1s were stained with the anti-TIM-1 polyclonal antibody and analyzed by flow cytometry (B) and the TIM-1 expression was quantified using MFI (C). Open and shaded histograms (B) indicate fluorescent intensity of TIM-1-expressing cells and vector-transduced control cells, respectively. (D,E) 293T cells expressing TIM-1s and control cells were infected with VSVΔG-EBOV, -RESTV, -MARV, -RAVV, and -LLOV GPs at a MOI of 0.02-0.04. The luciferase activity was measured 24 hours postinfection. The means and SDs of three independent experiments are shown. Significance was calculated using student's *t*-test (*$p < 0.05$, **$p < 0.01$).

Discussion

Several polymorphisms are found on amino acid sequences of the TIM-1 extracellular region consisting of the IgV and mucin domain in humans, mice, and monkeys[17, 32, 46, 47]. The polymorphisms based on deletions or insertions in the mucin domain are known to be associated with severity in several diseases, including asthma, allergic diseases and hepatitis A virus-induced liver disease[46, 47]. Since it was recently reported that the length of the mucin domain of TIM proteins regulates their ability to promote virus entry[51], the polymorphism in the mucin domain might regulate the function of TIM via a mechanism dependent on the length of the mucin domain. Other polymorphisms at N48 and K108 in the IgV region of TIM-1 were also found (Figure 14B)[17]. K108 has been shown to be responsible for the binding of anti-TIM-1 monoclonal antibody 190/4, which blocks hepatitis A virus infection, suggesting that K108 might be associated with the virus-recognition of TIM-1[17]. Here I focused on the other amino acid substitution at position 48 in the IgV domain and found that this mutation might regulate the activity of TIM-1s promoting filovirus cellular entry.

Although I found that the single amino acid residue at position 48 was responsible for the difference in the potential to promote infectivity of filoviruses between Vero E6 and COS-1 TIM-1s, the role of this particular amino acid in TIM-1-mediated viral entry remains unclear. Alanine scanning mutagenesis of the human TIM-1 IgV gene identified some important amino acid residues for TIM-1-mediated viral infection[52]: F55, R106, G111, N114, and D115 located on the CC' loop (44-64 aa) and FG loop (101-125 aa), which form the PtdSer-binding pocket. The crystal structure of the human TIM-1 IgV domain, predicted based on that of mouse TIM-1 using PHYRE2[52], revealed that the structure of the PtdSer-binding pocket was conserved between human and mouse TIM-

1s. I also predicted the crystal structures of the TIM-1 IgV domains of Vero E6 and COS-1 using the same approach and found that amino acids N48 and H48 were positioned on the edge of the CC' loop in the PtdSer-binding pocket and that this substitution did not seem to affect the structure of the PtdSer-binding pocket (Figure 18), suggesting that the amino acid substitution focused on in the present study might regulate the function of TIM-1 which affects the other viral entry step. Interestingly, I found that VLPs attached to 293T cells expressing Vero E6 TIM-1 less efficiently than cells expressing COS-1 TIM-1 (data not shown). Furthermore, I found that the interaction between MAb M224/1, which was shown to inhibit filovirus membrane fusion by interrupting the interplay between TIM-1 and NPC1 (see Chapter I), and TIM-1 was determined by the amino acid at position 48 in TIM-1 IgV domain (Figure 19). These findings suggest that the IgV domain including the amino acid at position 48 might be involved in not only viral attachment but also subsequent entry steps (e.g., viral internalization and membrane fusion).

Previous studies demonstrated that the human TIM-1 cytoplasmic tail was not required or nonessential to promote cellular entry of enveloped viruses, including EBOV[48, 51]. In this study, decreased ability to promote virus infectivity was observed in TIM-1 lacking its cytoplasmic tail, suggesting the involvement of the TIM-1 cytoplasmic tail in promoting virus entry, most likely through intracellular signaling pathways. The TIM-1 cytoplasmic tail has at least one tyrosine phosphorylation site that could potentiate the intracellular signaling regulating immune responses[16, 63, 69]. In addition, it has previously been reported that the TIM-1 tyrosine phosphorylation in its cytoplasmic tail activates the phosphatidylinositol 3-kinase pathway[15] that is responsible for macropinocytosis[5, 6]. Considering these findings together, I hypothesize that TIM-1-

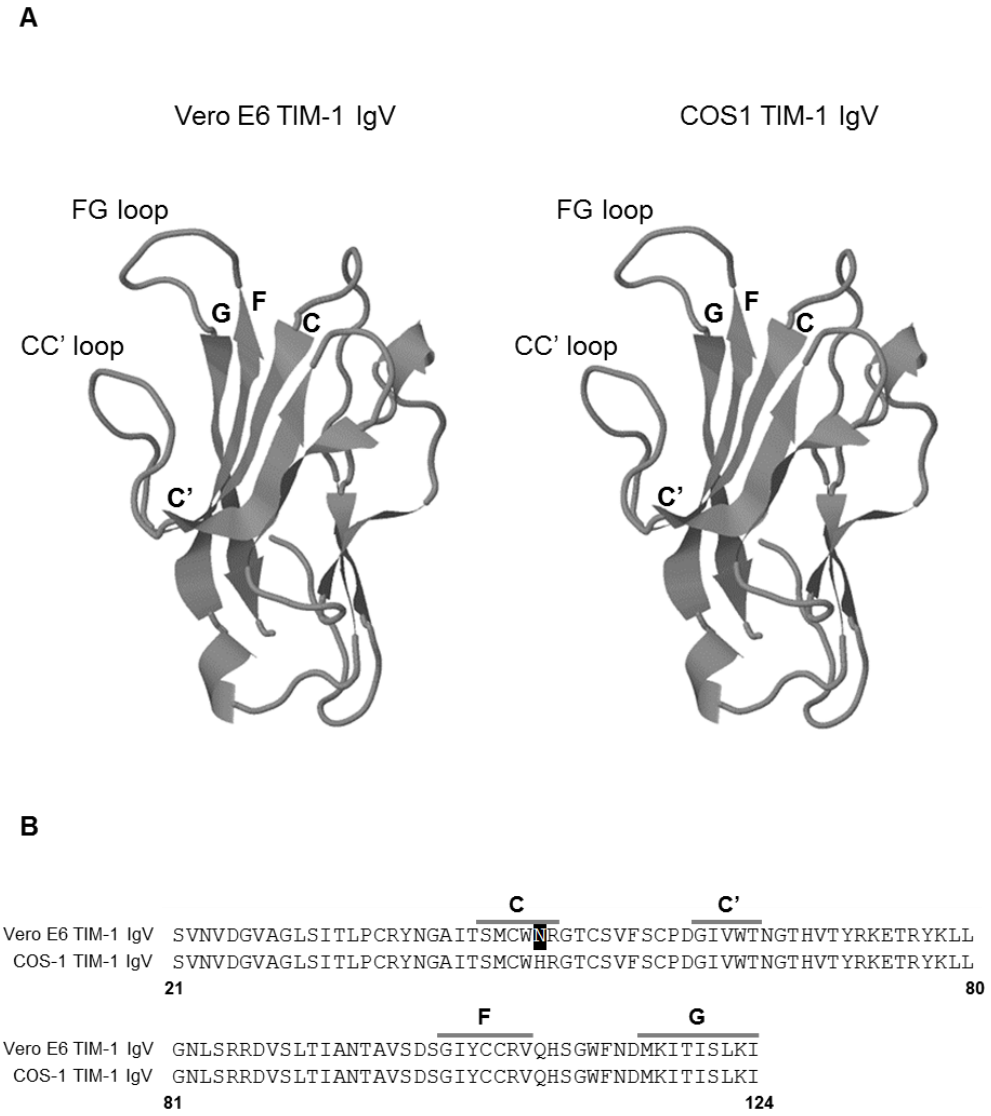

Figure 18. Crystal Structures of IgV domain of Vero E6 and COS-1 TIM-1. (A) Ribbon diagrams of IgV domain of Vero E6 TIM-1 (left panel) and COS-1 TIM-1 (right panel) are shown. β-sheets are labeled with their corresponding letters[65]. CC' loop (44-64 aa) and FG loop (101-125 aa) form the PtdSer-binding pocket. (B) The amino acid sequences of their IgV domain were aligned using GENETYX (version 10). Numbers of residues starting with the respective initiating methionine codons are shown[31]. β-sheets are marked above the alignment with lines and corresponding letters. Black shading indicates non-identical amino acid residues between Vero E6 and COS-1 TIM-1.

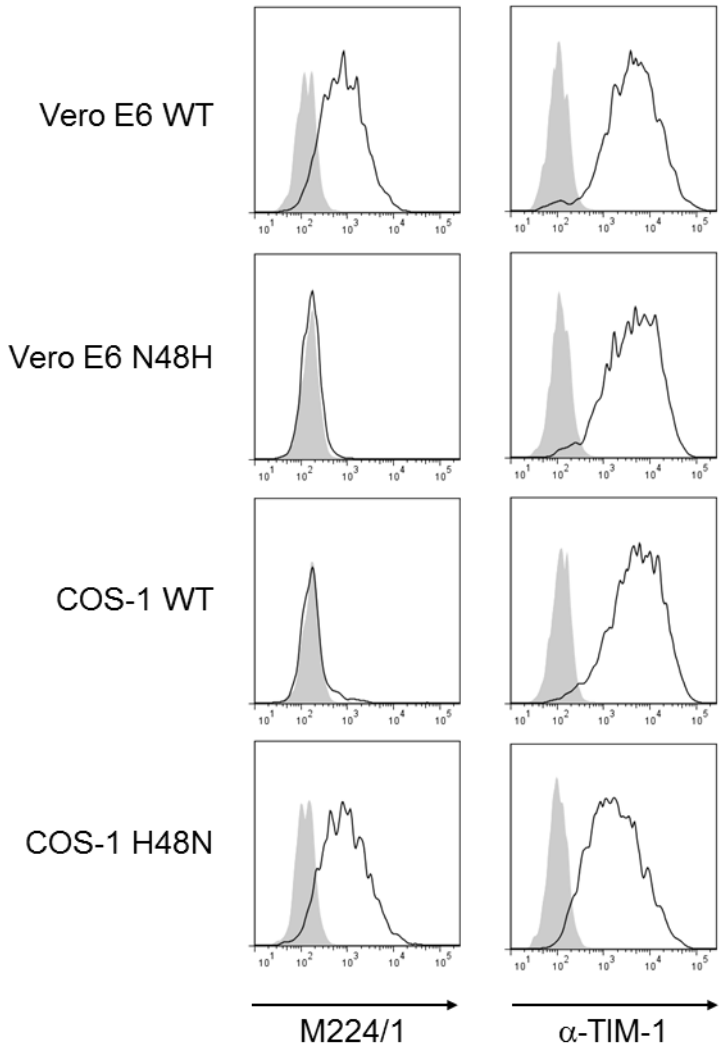

Figure 19. A single amino acid at position 48 in the TIM-1 IgV domain responsible for the interaction between MAb M224/1 and Vero E6 TIM-1. 293T cells expressing WT and mutant TIM-1s as indicated (see also Figure 17A) were stained with MAb M224/1 (black line, left panel), the anti-TIM-1 polyclonal antibody (black line, right panel), or their control antibodies (gray shading) and analyzed by flow cytometry.

induced signaling may partially contribute to enhanced viral uptake by macropinocytosis.

TIM-1 was shown to be highly expressed on injured kidney epithelial cells, activated CD4+ T cells, B cells, and mast cells[26, 35, 46, 63, 77]. Among these cells, kidney epithelial cells such as Vero E6 cells are highly susceptible to filovirus infection[35], but lymphocytes are resistant to filovirus infection although they express TIM-1[81], indicating that TIM-1 expression alone is not sufficient to confer susceptibility to filovirus infection. Furthermore, although ectopic expression of TIM-1 dramatically promoted filovirus GP-mediated entry into cells (Figure 17D and E)[28, 35, 52], filoviruses infect macrophages and dendritic cells, which have low or undetectable expression of TIM-1[19], suggesting that TIM-1 is not essential for filovirus infection. However, since filovirus antigens are detected in many organs, including the liver, spleen, kidneys, lymph nodes, and lungs at the late stage of infection[18], it is conceivable that TIM-1 polymorphism might affect overall disease progression in filovirus-infected individuals.

It has been demonstrated that TIM-1 directly binds to PtdSer on the viral envelope and TIM-1-mediated enhancement of viral infection has been reported in infection with several different enveloped viruses in a manner independent of specific receptor recognition by their envelope glycoproteins[28, 52, 53]. For example, TIM-1 enhances filovirus, alphavirus, flavivirus, and arenavirus infections but not Lassa virus, herpes simplex virus 1, influenza A virus (H7N1), and SARS coronavirus infections[28, 48, 52]. Interestingly, I found that the infectivities of VSVΔG-MARV GP and -RAVV GP were enhanced less efficiently by TIM-1 expression compared to VSVΔG-EBOV GP (Figure 17E). These findings suggest that there might be viral glycoprotein-dependent mechanisms underlying TIM-1-mediated viral entry. Thus, further studies are needed to fully understand the contribution of TIM-1 to the tissue tropism and pathogenicity of

enveloped viruses.

Summary

Filoviruses, including Ebola and Marburg viruses, cause severe hemorrhagic fever in humans and nonhuman primates with mortality rates of up to 90%. Human TIM-1 is one of the host proteins that have been shown to promote filovirus entry into cells. In this study, I cloned TIM-1 genes from three different African green monkey kidney cell lines (Vero E6, COS-1, and BSC-1) and found that TIM-1 of Vero E6 had deletions (1 and 23 amino acids) and 6 amino acid substitutions compared with those of COS-1 and BSC-1. Interestingly, Vero E6 TIM-1 had a greater ability to promote the infectivity of vesicular stomatitis viruses pseudotyped with filovirus glycoproteins than COS-1-derived TIM-1. I further found that the increased ability of Vero E6 TIM-1 to promote virus infectivity was most likely due to a single amino acid difference between these TIM-1s. These results suggest that a polymorphism of the TIM-1 molecules is one of the factors that influence cell susceptibility to filovirus infection, providing a new insight into the molecular basis for the filovirus host range.

Conclusion

Filoviruses including Ebola and Marburg viruses cause rapidly fatal disease characterized by severe hemorrhagic manifestations in humans and nonhuman primates. Consequently, filovirus infections continue to assault human populations, as demonstrated by a recent outbreak in West Africa. Despite extensive research, there are currently no approved vaccines or therapeutics against these viruses. In general, the cellular entry step of viruses is one of the key mechanisms to develop antiviral strategies and the receptor preference is often control susceptibility of host cells to viruses. It has been demonstrated that filoviruses utilize multiple host molecules for entry into cells. However, molecular mechanisms underlying the entry process have not been fully understood, while TIM-1 and NPC1 are thought to serve as attachment and fusion receptors for filoviruses, respectively.

In chapter I, I demonstrated that TIM-1 was involved in not only filovirus attachment but also subsequent steps of viral entry through the interaction with NPC1 and that their interplay was important for efficient membrane fusion. Moreover, I showed that filovirus infection and GP-mediated membrane fusion in cultured cells were remarkably suppressed by the treatment with a TIM-1-specific MAb M224/1 that interfered with the interaction between TIM-1 and NPC1. In chapter II, I found that Vero E6 TIM-1 had different primary structures and a greater ability to promote infectivity of VSVs pseudotyped with filovirus GPs, compared with TIM-1s derived from the other African green monkey kidney cell lines tested. These results suggest that a polymorphism of the TIM-1 molecules is one of the factors that influence the cell susceptibility to filovirus infection.

The present study provides the first evidence that the interaction between these attachment and fusion receptors is important for filovirus infection, demonstrating an attractive cellular target of antiviral strategies. The detailed structural basis on the molecular interface of the interactions between TIM-1 and NPC1 may provide new insights into the development of antivirals such as low-molecular-weight compounds that can be universally used against filovirus infections. Furthermore, it was also newly suggested that polymorphisms of host molecules might be involved in cell susceptibility to filovirus infection, providing a new insight into the molecular basis for the filovirus host range.

Acknowledgements

I would like to express my sincere gratitude to my boss, Prof. Ayato Takada (Division of Global Epidemiology, Hokkaido University Research Center for Zoonosis Control, Sapporo, Japan). He gave me generous support for my experiments, innumerable accurate advice and guidance during my course and a lot of opportunities for growth.

My heartfelt appreciation for their helpful advice and suggestions goes to Prof. Hirofumi Sawa (Division of Molecular Pathobiology, Hokkaido University Research Center for Zoonosis Control, Sapporo, Japan), Prof. Yasuhiko Suzuki (Division of Bioresources, Hokkaido University Research Center for Zoonosis Control, Sapporo, Japan), and Prof. Hideaki Higashi (Division of Infection and Immunity, Hokkaido University Research Center for Zoonosis Control, Sapporo, Japan).

I would like to offer my special thanks to Associate Prof. Manabu Igarashi and Specially Appointed Assistant Prof. Reiko Yoshida (Division of Global Epidemiology, Hokkaido University Research Center for Zoonosis Control, Sapporo, Japan) for their kind and helpful guidance.

I am deeply grateful to Dr. Daisuke Fujikura (Division of Infection and Immunity, Hokkaido University Research Center for Zoonosis Control, Sapporo, Japan) and Associate Prof. Asuka Nanbo (Department of Cell Physiology, Hokkaido University Graduate School of Medicine, Sapporo, Japan) for their technical assistance, intellectual advice, and warm support.

I would like to thank Dr. Andrea Marzi, Dr. Heinz Feldmann, Dr. Shelly Robertson, Dr. Hideki Ebihara, Ms. Key Menk, Dr. Keita Matsuno, Dr. Atsushi Okumura (Laboratory of Virology, Division of Intramural Research, National Institute of Allergy and Infectious Diseases, National Institutes of Health, Rocky Mountain Laboratories, Hamilton, Montana, USA), Dr. Yoshimi Tsuda (Department of Microbiology, Hokkaido University Graduate School of Medicine, Sapporo, Japan), and Dr. Eri Saijo (Laboratory of Persistent Viral Diseases, Division of Intramural Research, National Institute of Allergy and Infectious Diseases, National Institutes of Health, Rocky Mountain Laboratories, Hamilton, Montana, USA) for their expertise and advice and cordial welcome during my stay in Hamilton, providing much valuable experience.

The following people helpfully provided technical and academic advice and support: Prof. Kimihito Ito (Division of Bioinformatics, Hokkaido University Research Center for Zoonosis Control, Sapporo, Japan), Dr. Rashid Manzoor, Dr. Masahiro Kajihara, Mr. Junki Maruyama, Ms. Hiroko Miyamoto, Ms. Mari Ishijima (Division of Global Epidemiology, Hokkaido University Research Center for Zoonosis Control, Sapporo, Japan), Dr. Osamu Noyori (Department of Infectious Diseases, Kyoto Prefectural University of Medicine, Kyoto, Japan), and Dr. Eri Nakayama (Department of Virology 1, National Institute of Infectious Disease, Tokyo, Japan). I also received kind daily support from Dr. Mieko Muramatsu, Mr. Naganori Nao, Ms. Wakako Furuyama, Mr. Nao Eguchi, Ms. Akina Mori, and Ms. Ichiko Sawada (Division of Global Epidemiology, Hokkaido University Research Center for Zoonosis Control, Sapporo, Japan).

Special thanks to my schoolfellows, Kanjana Changkaew (Division of Bioresources, Hokkaido University Research Center for Zoonosis Control, Sapporo, Japan), Mr. Yongjin Qiu (Division of Collaboration and Education, Hokkaido University Research Center for Zoonosis Control, Sapporo, Japan), and Mr. Keisuke Aoshima (Laboratory of Comparative Pathology, Department of Veterinary Clinical Sciences, Hokkaido University Graduate School of Veterinary Medicine, Sapporo, Japan) for their help and encouragement during my course. I would also like to thank all members of the Hokkaido University Research Center for Zoonosis Control for their help and kindness.

Finally, I can never express my gratitude enough for all my family members have done for me. I owe my life to them.

和文要旨

フィロウイルス科に属するエボラウイルス及びマールブルグウイルスはヒトを含む霊長類動物に感染し、重篤な出血熱を引き起こす病原体として知られている。現在、フィロウイルス感染症に対する治療薬や予防法として承認されたものはなく、それらの開発が急がれている。感染の第一ステップである細胞侵入過程はウイルス粒子表面糖タンパク質（GP）依存的であり、効果的な予防・治療薬開発のための有力な標的メカニズムの一つとして挙げられる。これまでに、フィロウイルスの細胞への吸着及び膜融合に関与する様々な宿主分子が報告されている一方、その分子メカニズムには不明な点が多い。

第一章では、フィロウイルスの細胞侵入過程におけるウイルス及び宿主分子の相互作用の解明を目的として、フィロウイルスの細胞侵入を阻害するモノクローナル抗体 M224/1 の阻害メカニズムを解析した。M224/1 は、フィロウイルスに対して高い感受性を示すアフリカミドリザル腎臓上皮細胞 Vero E6 を抗原としてマウスを免疫し、誘導された抗 Vero E6 抗体の中から、水泡性口炎ウイルス（VSV）の G タンパク質をエボラウイルスの GP に置換したシュードタイプウイルスの Vero E6 への感染阻害効率を指標としたスクリーニングにより得られた。M224/1 による感染阻害効果は、実際のエボラウイルス及びマールブルグウイルスに対しても認められた。Vero E6 の RNA から作製した完全長 cDNA ライブラリーを、M224/1 が結合しない Jurkat T 細胞にレトロウイルスベクターによって導入し、M224 が結合するようになった細胞をクローニングした

結果、M224/1 の標的分子が T cell immunoglobulin and Mucin domain 1（TIM-1）であることが明らかとなった。TIM-1 は細胞外領域に機能ドメインである IgV をもつ I 型の膜タンパク質であり、フィロウイルスの細胞への吸着に関与する分子として知られており、M224/1 は IgV ドメインに結合することが示された。次に、M224/1 存在下及び非存在下で、蛍光標識したウイルス様粒子（VLP）の吸着・取り込み・膜融合を定量的に比較解析した結果、M224/1 存在下での VLP の細胞への吸着阻害効果は僅かであるが、VLP とエンドソーム膜との膜融合が著しく阻害されることが明らかとなった。そこで、フィロウイルスの膜融合に必須である宿主分子 Niemann-Pick C1（NPC1）と TIM-1 の Vero E6 細胞内局在を蛍光顕微鏡で観察したところ、核近傍に集積する細胞内小胞において両者の共局在が認められた。さらに、293T 細胞での過剰発現系を用いた免疫沈降法により、TIM-1 と NPC1 が結合することが明らかとなった。細胞内での TIM-1/NPC1 複合体の局在は、蛍光タンパク質再構成法（BiFC: bimolecular fluorescence complementation）によっても確認された。興味深いことに、M224/1 は TIM-1/NPC1 複合体形成を濃度依存的に抑制した。さらに、細胞内の TIM-1/NPC1 複合体と膜融合を起こしている VLP を蛍光顕微鏡で観察したところ、両者の局在は一致した。以上の結果より、フィロウイルスは TIM-1 を介して細胞表面に吸着した後、TIM-1 と共に細胞内に取り込まれ、後期エンドソーム/リソソームにおいて、TIM-1 と NPC1 との相互作用を経て膜融合を行い、細胞内に侵入することが示唆された。

第二章では、フィロウイルス感受性に対する TIM-1 多型の影響について解析した。フィロウイルスの感染実験には Vero E6 の他にも複数のアフリカミ

ドリザル腎臓上皮由来の細胞株（COS-1、BSC-1 等）が用いられている。しかし、これらの細胞間でのウイルス感受性や受容体の発現パターンなどの違いに関する情報は少ない。本章では、これらの細胞に発現する TIM-1 に焦点を当て、フィロウイルスに対する TIM-1 発現細胞の感受性について比較解析した。まず、COS-1 及び BSC-1 より TIM-1 遺伝子のクローニングを行い、アミノ酸配列を比較した結果、Vero E6 は他の細胞株とは一部アミノ酸配列が異なる TIM-1 を発現していることが分かった。次に、それぞれの TIM-1 を安定に発現する細胞を作製し、VSV シュードタイプウイルスに対する細胞の感受性を比較したところ、Vero E6 由来 TIM-1 発現 293T 細胞のウイルス感受性は他の細胞由来 TIM-1 発現 293T 細胞よりも有意に高かった。IgV ドメインのアミノ酸配列を比較すると、48 番目のアミノ酸（Vero E6：アスパラギン、COS-1, BSC-1：ヒスチジン）が異なっていた。この 48 番目のアミノ酸を相互に置換した TIM-1 を作製し、野生型及び変異型 TIM-1 を発現する細胞間でのウイルス感受性を比較した。その結果、異なる TIM-1 間でみられた感受性増強効果の違いがこの IgV ドメイン中の 1 アミノ酸の違いに依存することが分かった。この 48 番目のアミノ酸の違いによる感受性の変化はフィロウイルス科全てのウイルス属において認められた。以上より、TIM-1 の多型がフィロウイルス感受性を左右する要因の一つであることが示唆された。

本研究によって、TIM-1 がウイルス粒子の細胞への吸着だけでなく、エンベロープとエンドソーム膜の融合においても重要であることが示された。また、M224/1 が TIM-1 と NPC1 の結合を阻害することにより、フィロウイルスの

膜融合を抑制することから、ウイルスの細胞侵入過程におけるこれらの宿主タンパク質間の結合阻害はフィロウイルス感染症に対する予防・治療法の新たな標的になることが期待される。さらに本研究では、宿主分子の多型が宿主細胞のフィロウイルス感受性に関与する可能性を初めて示した。これらの新しい知見は、フィロウイルスの細胞侵入機構、宿主域、組織特異性、さらには病原性発現機構の分子メカニズム解明に繋がるとともに、フィロウイルスによる感染症の予防・治療法の開発に大きく貢献すると期待される。

References

1) Aleksandrowicz, P., Marzi, A., Biedenkopf, N., Beimforde, N., Becker, S., Hoenen, T., Feldmann, H. and Schnittler, H. J. 2011. Ebola virus enters host cells by macropinocytosis and clathrin-mediated endocytosis. *The Journal of infectious diseases,* **204 Suppl 3**: S957-967.

2) Allela, L., Boury, O., Pouillot, R., Delicat, A., Yaba, P., Kumulungui, B., Rouquet, P., Gonzalez, J. P. and Leroy, E. M. 2005. Ebola virus antibody prevalence in dogs and human risk. *Emerging infectious diseases,* **11**: 385-390.

3) Alvarez, C. P., Lasala, F., Carrillo, J., Muniz, O., Corbi, A. L. and Delgado, R. 2002. C-type lectins DC-SIGN and L-SIGN mediate cellular entry by Ebola virus in cis and in trans. *Journal of virology,* **76**: 6841-6844.

4) Amman, B. R., Carroll, S. A., Reed, Z. D., Sealy, T. K., Balinandi, S., Swanepoel, R., Kemp, A., Erickson, B. R., Comer, J. A., Campbell, S., Cannon, D. L., Khristova, M. L., Atimnedi, P., Paddock, C. D., Crockett, R. J., Flietstra, T. D., Warfield, K. L., Unfer, R., Katongole-Mbidde, E., Downing, R., Tappero, J. W., Zaki, S. R., Rollin, P. E., Ksiazek, T. G., Nichol, S. T. and Towner, J. S. 2012. Seasonal pulses of Marburg virus circulation in juvenile Rousettus aegyptiacus bats coincide with periods of increased risk of human infection. *PLoS pathogens,* **8**: e1002877.

5) Amyere, M., Payrastre, B., Krause, U., Van Der Smissen, P., Veithen, A. and Courtoy, P. J. 2000. Constitutive macropinocytosis in oncogene-transformed fibroblasts depends on sequential permanent activation of phosphoinositide 3-kinase and phospholipase C. *Mol Biol Cell*, **11**: 3453-3467.

6) Araki, N., Johnson, M. T. and Swanson, J. A. 1996. A role for phosphoinositide 3-kinase in the completion of macropinocytosis and phagocytosis by macrophages. *Journal of Cell Biology*, **135**: 1249-1260.

7) Balasubramanian, S., Kota, S. K., Kuchroo, V. K., Humphreys, B. D. and Strom, T. B. 2012. TIM family proteins promote the lysosomal degradation of the nuclear receptor NUR77. *Science signaling*, **5**: ra90.

8) Barrette, R. W., Metwally, S. A., Rowland, J. M., Xu, L., Zaki, S. R., Nichol, S. T., Rollin, P. E., Towner, J. S., Shieh, W. J., Batten, B., Sealy, T. K., Carrillo, C., Moran, K. E., Bracht, A. J., Mayr, G. A., Sirios-Cruz, M., Catbagan, D. P., Lautner, E. A., Ksiazek, T. G., White, W. R. and McIntosh, M. T. 2009. Discovery of swine as a host for the Reston ebolavirus. *Science*, **325**: 204-206.

9) Becker, S., Spiess, M. and Klenk, H. D. 1995. The asialoglycoprotein receptor is a potential liver-specific receptor for Marburg virus. *The Journal of general virology*, **76 (Pt 2)**: 393-399.

10) Bukreyev, A. A., Chandran, K., Dolnik, O., Dye, J. M., Ebihara, H., Leroy, E. M., Muhlberger, E., Netesov, S. V., Patterson, J. L., Paweska, J. T., Saphire, E. O., Smither, S. J., Takada, A., Towner, J. S., Volchkov, V. E., Warren, T. K. and Kuhn, J. H. 2014. Discussions and decisions of the 2012-2014 International Committee on Taxonomy of Viruses (ICTV) Filoviridae Study Group, January 2012-June 2013. *Archives of virology*, **159**: 821-830.

11) Carette, J. E., Raaben, M., Wong, A. C., Herbert, A. S., Obernosterer, G., Mulherkar, N., Kuehne, A. I., Kranzusch, P. J., Griffin, A. M., Ruthel, G., Dal Cin, P., Dye, J. M., Whelan, S. P., Chandran, K. and Brummelkamp, T. R. 2011. Ebola virus entry requires the cholesterol transporter Niemann-Pick C1. *Nature*,

477: 340-343.

12) Chandran, K., Sullivan, N. J., Felbor, U., Whelan, S. P. and Cunningham, J. M. 2005. Endosomal proteolysis of the Ebola virus glycoprotein is necessary for infection. *Science*, **308**: 1643-1645.

13) Changula, K., Yoshida, R., Noyori, O., Marzi, A., Miyamoto, H., Ishijima, M., Yokoyama, A., Kajihara, M., Feldmann, H., Mweene, A. S. and Takada, A. 2013. Mapping of conserved and species-specific antibody epitopes on the Ebola virus nucleoprotein. *Virus research*, **176**: 83-90.

14) Cote, M., Misasi, J., Ren, T., Bruchez, A., Lee, K., Filone, C. M., Hensley, L., Li, Q., Ory, D., Chandran, K. and Cunningham, J. 2011. Small molecule inhibitors reveal Niemann-Pick C1 is essential for Ebola virus infection. *Nature*, **477**: 344-348.

15) de Souza, A. J., Oak, J. S., Jordanhazy, R., DeKruyff, R. H., Fruman, D. A. and Kane, L. P. 2008. T cell Ig and mucin domain-1-mediated T cell activation requires recruitment and activation of phosphoinositide 3-kinase. *Journal of immunology*, **180**: 6518-6526.

16) de Souza, A. J., Oriss, T. B., O'Malley, K. J., Ray, A. and Kane, L. P. 2005. T cell Ig and mucin 1 (TIM-1) is expressed on in vivo-activated T cells and provides a costimulatory signal for T cell activation. *Proceedings of the National Academy of Sciences of the United States of America*, **102**: 17113-17118.

17) Feigelstock, D., Thompson, P., Mattoo, P. and Kaplan, G. G. 1998. Polymorphisms of the hepatitis A virus cellular receptor 1 in African green monkey kidney cells result in antigenic variants that do not react with protective monoclonal antibody 190/4. *Journal of virology*, **72**: 6218-6222.

18) Feldmann, H. and Klenk, H. D. 1996. Filoviruses. In: *Medical Microbiology*, 4th ed., Baron, S. ed., Galveston (TX).

19) Geisbert, T. W. and Hensley, L. E. 2004. Ebola virus: new insights into disease aetiopathology and possible therapeutic interventions. *Expert reviews in molecular medicine*, **6**: 1-24.

20) Gramberg, T., Hofmann, H., Moller, P., Lalor, P. F., Marzi, A., Geier, M., Krumbiegel, M., Winkler, T., Kirchhoff, F., Adams, D. H., Becker, S., Munch, J. and Pohlmann, S. 2005. LSECtin interacts with filovirus glycoproteins and the spike protein of SARS coronavirus. *Virology*, **340**: 224-236.

21) Hashimoto, J., Watanabe, T., Seki, T., Karasawa, S., Izumikawa, M., Seki, T., Iemura, S., Natsume, T., Nomura, N., Goshima, N., Miyawaki, A., Takagi, M. and Shin-Ya, K. 2009. Novel in vitro protein fragment complementation assay applicable to high-throughput screening in a 1536-well format. *Journal of biomolecular screening*, **14**: 970-979.

22) Higgins, M. E., Davies, J. P., Chen, F. W. and Ioannou, Y. A. 1999. Niemann-Pick C1 is a late endosome-resident protein that transiently associates with lysosomes and the trans-Golgi network. *Molecular genetics and metabolism*, **68**: 1-13.

23) Hoekstra, D., de Boer, T., Klappe, K. and Wilschut, J. 1984. Fluorescence method for measuring the kinetics of fusion between biological membranes. *Biochemistry*, **23**: 5675-5681.

24) Hofmann-Winkler, H., Kaup, F. and Pohlmann, S. 2012. Host cell factors in filovirus entry: novel players, new insights. *Viruses*, **4**: 3336-3362.

25) Ichimura, T., Asseldonk, E. J., Humphreys, B. D., Gunaratnam, L., Duffield, J.

S. and Bonventre, J. V. 2008. Kidney injury molecule-1 is a phosphatidylserine receptor that confers a phagocytic phenotype on epithelial cells. *The Journal of clinical investigation*, **118**: 1657-1668.

26) Ichimura, T., Bonventre, J. V., Bailly, V., Wei, H., Hession, C. A., Cate, R. L. and Sanicola, M. 1998. Kidney injury molecule-1 (KIM-1), a putative epithelial cell adhesion molecule containing a novel immunoglobulin domain, is up-regulated in renal cells after injury. *The Journal of biological chemistry*, **273**: 4135-4142.

27) Ito, H., Watanabe, S., Sanchez, A., Whitt, M. A. and Kawaoka, Y. 1999. Mutational analysis of the putative fusion domain of Ebola virus glycoprotein. *Journal of virology*, **73**: 8907-8912.

28) Jemielity, S., Wang, J. J., Chan, Y. K., Ahmed, A. A., Li, W., Monahan, S., Bu, X., Farzan, M., Freeman, G. J., Umetsu, D. T., Dekruyff, R. H. and Choe, H. 2013. TIM-family proteins promote infection of multiple enveloped viruses through virion-associated phosphatidylserine. *PLoS pathogens*, **9**: e1003232.

29) Kajihara, M., Marzi, A., Nakayama, E., Noda, T., Kuroda, M., Manzoor, R., Matsuno, K., Feldmann, H., Yoshida, R., Kawaoka, Y. and Takada, A. 2012. Inhibition of Marburg virus budding by nonneutralizing antibodies to the envelope glycoprotein. *Journal of virology*, **86**: 13467-13474.

30) Kajihara, M., Nakayama, E., Marzi, A., Igarashi, M., Feldmann, H. and Takada, A. 2013. Novel mutations in Marburg virus glycoprotein associated with viral evasion from antibody mediated immune pressure. *The Journal of general virology*, **94**: 876-883.

31) Kaplan, G., Totsuka, A., Thompson, P., Akatsuka, T., Moritsugu, Y. and Feinstone, S. M. 1996. Identification of a surface glycoprotein on African green

monkey kidney cells as a receptor for hepatitis A virus. *The EMBO journal*, **15**: 4282-4296.

32) Kim, H. Y., Eyheramonho, M. B., Pichavant, M., Gonzalez Cambaceres, C., Matangkasombut, P., Cervio, G., Kuperman, S., Moreiro, R., Konduru, K., Manangeeswaran, M., Freeman, G. J., Kaplan, G. G., DeKruyff, R. H., Umetsu, D. T. and Rosenzweig, S. D. 2011. A polymorphism in TIM1 is associated with susceptibility to severe hepatitis A virus infection in humans. *The Journal of clinical investigation*, **121**: 1111-1118.

33) Kitamura, T., Koshino, Y., Shibata, F., Oki, T., Nakajima, H., Nosaka, T. and Kumagai, H. 2003. Retrovirus-mediated gene transfer and expression cloning: powerful tools in functional genomics. *Experimental hematology*, **31**: 1007-1014.

34) Kobayashi, N., Karisola, P., Pena-Cruz, V., Dorfman, D. M., Jinushi, M., Umetsu, S. E., Butte, M. J., Nagumo, H., Chernova, I., Zhu, B., Sharpe, A. H., Ito, S., Dranoff, G., Kaplan, G. G., Casasnovas, J. M., Umetsu, D. T., Dekruyff, R. H. and Freeman, G. J. 2007. TIM-1 and TIM-4 glycoproteins bind phosphatidylserine and mediate uptake of apoptotic cells. *Immunity*, **27**: 927-940.

35) Kondratowicz, A. S., Lennemann, N. J., Sinn, P. L., Davey, R. A., Hunt, C. L., Moller-Tank, S., Meyerholz, D. K., Rennert, P., Mullins, R. F., Brindley, M., Sandersfeld, L. M., Quinn, K., Weller, M., McCray, P. B., Jr., Chiorini, J. and Maury, W. 2011. T-cell immunoglobulin and mucin domain 1 (TIM-1) is a receptor for Zaire Ebolavirus and Lake Victoria Marburgvirus. *Proceedings of the National Academy of Sciences of the United States of America*, **108**: 8426-

8431.

36) Lasala, F., Arce, E., Otero, J. R., Rojo, J. and Delgado, R. 2003. Mannosyl glycodendritic structure inhibits DC-SIGN-mediated Ebola virus infection in cis and in trans. *Antimicrobial agents and chemotherapy*, **47**: 3970-3972.

37) Lee, J. E., Fusco, M. L., Hessell, A. J., Oswald, W. B., Burton, D. R. and Saphire, E. O. 2008. Structure of the Ebola virus glycoprotein bound to an antibody from a human survivor. *Nature*, **454**: 177-182.

38) Leroy, E. M., Kumulungui, B., Pourrut, X., Rouquet, P., Hassanin, A., Yaba, P., Delicat, A., Paweska, J. T., Gonzalez, J. P. and Swanepoel, R. 2005. Fruit bats as reservoirs of Ebola virus. *Nature*, **438**: 575-576.

39) Leroy, E. M., Rouquet, P., Formenty, P., Souquiere, S., Kilbourne, A., Froment, J. M., Bermejo, M., Smit, S., Karesh, W., Swanepoel, R., Zaki, S. R. and Rollin, P. E. 2004. Multiple Ebola virus transmission events and rapid decline of central African wildlife. *Science*, **303**: 387-390.

40) Licata, J. M., Johnson, R. F., Han, Z. and Harty, R. N. 2004. Contribution of ebola virus glycoprotein, nucleoprotein, and VP24 to budding of VP40 virus-like particles. *Journal of virology*, **78**: 7344-7351.

41) Lin, G., Simmons, G., Pohlmann, S., Baribaud, F., Ni, H., Leslie, G. J., Haggarty, B. S., Bates, P., Weissman, D., Hoxie, J. A. and Doms, R. W. 2003. Differential N-linked glycosylation of human immunodeficiency virus and Ebola virus envelope glycoproteins modulates interactions with DC-SIGN and DC-SIGNR. *Journal of virology*, **77**: 1337-1346.

42) Maruyama, J., Miyamoto, H., Kajihara, M., Ogawa, H., Maeda, K., Sakoda, Y., Yoshida, R. and Takada, A. 2014. Characterization of the envelope glycoprotein

of a novel filovirus, lloviu virus. *Journal of virology*, **88**: 99-109.

43) Marzi, A., Gramberg, T., Simmons, G., Moller, P., Rennekamp, A. J., Krumbiegel, M., Geier, M., Eisemann, J., Turza, N., Saunier, B., Steinkasserer, A., Becker, S., Bates, P., Hofmann, H. and Pohlmann, S. 2004. DC-SIGN and DC-SIGNR interact with the glycoprotein of Marburg virus and the S protein of severe acute respiratory syndrome coronavirus. *Journal of virology*, **78**: 12090-12095.

44) Matsuno, K., Kishida, N., Usami, K., Igarashi, M., Yoshida, R., Nakayama, E., Shimojima, M., Feldmann, H., Irimura, T., Kawaoka, Y. and Takada, A. 2010. Different potential of C-type lectin-mediated entry between Marburg virus strains. *Journal of virology*, **84**: 5140-5147.

45) McIntire, J. J., Umetsu, D. T. and DeKruyff, R. H. 2004. TIM-1, a novel allergy and asthma susceptibility gene. *Springer seminars in immunopathology*, **25**: 335-348.

46) McIntire, J. J., Umetsu, S. E., Akbari, O., Potter, M., Kuchroo, V. K., Barsh, G. S., Freeman, G. J., Umetsu, D. T. and DeKruyff, R. H. 2001. Identification of Tapr (an airway hyperreactivity regulatory locus) and the linked Tim gene family. *Nature immunology*, **2**: 1109-1116.

47) McIntire, J. J., Umetsu, S. E., Macaubas, C., Hoyte, E. G., Cinnioglu, C., Cavalli-Sforza, L. L., Barsh, G. S., Hallmayer, J. F., Underhill, P. A., Risch, N. J., Freeman, G. J., DeKruyff, R. H. and Umetsu, D. T. 2003. Immunology: hepatitis A virus link to atopic disease. *Nature*, **425**: 576.

48) Meertens, L., Carnec, X., Lecoin, M. P., Ramdasi, R., Guivel-Benhassine, F., Lew, E., Lemke, G., Schwartz, O. and Amara, A. 2012. The TIM and TAM

families of phosphatidylserine receptors mediate dengue virus entry. *Cell host & microbe*, **12**: 544-557.

49) Miller, E. H., Obernosterer, G., Raaben, M., Herbert, A. S., Deffieu, M. S., Krishnan, A., Ndungo, E., Sandesara, R. G., Carette, J. E., Kuehne, A. I., Ruthel, G., Pfeffer, S. R., Dye, J. M., Whelan, S. P., Brummelkamp, T. R. and Chandran, K. 2012. Ebola virus entry requires the host-programmed recognition of an intracellular receptor. *The EMBO journal*, **31**: 1947-1960.

50) Misasi, J., Chandran, K., Yang, J. Y., Considine, B., Filone, C. M., Cote, M., Sullivan, N., Fabozzi, G., Hensley, L. and Cunningham, J. 2012. Filoviruses require endosomal cysteine proteases for entry but exhibit distinct protease preferences. *Journal of virology*, **86**: 3284-3292.

51) Moller-Tank, S., Albritton, L. M., Rennert, P. D. and Maury, W. 2014. Characterizing functional domains for TIM-mediated enveloped virus entry. *Journal of virology*, **88**: 6702-6713.

52) Moller-Tank, S., Kondratowicz, A. S., Davey, R. A., Rennert, P. D. and Maury, W. 2013. Role of the phosphatidylserine receptor TIM-1 in enveloped-virus entry. *Journal of virology*, **87**: 8327-8341.

53) Morizono, K. and Chen, I. S. 2014. Role of phosphatidylserine receptors in enveloped virus infection. *Journal of virology*, **88**: 4275-4290.

54) Morizono, K., Xie, Y., Olafsen, T., Lee, B., Dasgupta, A., Wu, A. M. and Chen, I. S. 2011. The soluble serum protein Gas6 bridges virion envelope phosphatidylserine to the TAM receptor tyrosine kinase Axl to mediate viral entry. *Cell host & microbe*, **9**: 286-298.

55) Nakayama, E., Tomabechi, D., Matsuno, K., Kishida, N., Yoshida, R.,

Feldmann, H. and Takada, A. 2011. Antibody-dependent enhancement of Marburg virus infection. *The Journal of infectious diseases*, **204 Suppl 3**: S978-985.

56) Nanbo, A., Imai, M., Watanabe, S., Noda, T., Takahashi, K., Neumann, G., Halfmann, P. and Kawaoka, Y. 2010. Ebolavirus is internalized into host cells via macropinocytosis in a viral glycoprotein-dependent manner. *PLoS pathogens*, **6**: e1001121.

57) Negredo, A., Palacios, G., Vazquez-Moron, S., Gonzalez, F., Dopazo, H., Molero, F., Juste, J., Quetglas, J., Savji, N., de la Cruz Martinez, M., Herrera, J. E., Pizarro, M., Hutchison, S. K., Echevarria, J. E., Lipkin, W. I. and Tenorio, A. 2011. Discovery of an ebolavirus-like filovirus in europe. *PLoS pathogens*, **7**: e1002304.

58) Neufeld, E. B., Wastney, M., Patel, S., Suresh, S., Cooney, A. M., Dwyer, N. K., Roff, C. F., Ohno, K., Morris, J. A., Carstea, E. D., Incardona, J. P., Strauss, J. F., 3rd, Vanier, M. T., Patterson, M. C., Brady, R. O., Pentchev, P. G. and Blanchette-Mackie, E. J. 1999. The Niemann-Pick C1 protein resides in a vesicular compartment linked to retrograde transport of multiple lysosomal cargo. *The Journal of biological chemistry*, **274**: 9627-9635.

59) Noda, T., Sagara, H., Suzuki, E., Takada, A., Kida, H. and Kawaoka, Y. 2002. Ebola virus VP40 drives the formation of virus-like filamentous particles along with GP. *Journal of virology*, **76**: 4855-4865.

60) Pan, Y., Zhang, W., Cui, L., Hua, X., Wang, M. and Zeng, Q. 2014. Reston virus in domestic pigs in China. *Archives of virology*, **159**: 1129-1132.

61) Patel, S. C., Suresh, S., Kumar, U., Hu, C. Y., Cooney, A., Blanchette-Mackie, E.

J., Neufeld, E. B., Patel, R. C., Brady, R. O., Patel, Y. C., Pentchev, P. G. and Ong, W. Y. 1999. Localization of Niemann-Pick C1 protein in astrocytes: implications for neuronal degeneration in Niemann- Pick type C disease. *Proceedings of the National Academy of Sciences of the United States of America*, **96**: 1657-1662.

62) Reed, L. J. and Muench, H. 1938. A simple method of estimating fifty percent endopiont. *American Journal of Epidemiology*, **27**: 493-497.

63) Rennert, P. D. 2011. Novel roles for TIM-1 in immunity and infection. *Immunology letters*, **141**: 28-35.

64) Saeed, M. F., Kolokoltsov, A. A., Albrecht, T. and Davey, R. A. 2010. Cellular entry of ebola virus involves uptake by a macropinocytosis-like mechanism and subsequent trafficking through early and late endosomes. *PLoS pathogens*, **6**: e1001110.

65) Santiago, C., Ballesteros, A., Tami, C., Martinez-Munoz, L., Kaplan, G. G. and Casasnovas, J. M. 2007. Structures of T Cell immunoglobulin mucin receptors 1 and 2 reveal mechanisms for regulation of immune responses by the TIM receptor family. *Immunity*, **26**: 299-310.

66) Schornberg, K., Matsuyama, S., Kabsch, K., Delos, S., Bouton, A. and White, J. 2006. Role of endosomal cathepsins in entry mediated by the Ebola virus glycoprotein. *Journal of virology*, **80**: 4174-4178.

67) Seitz, H. M., Camenisch, T. D., Lemke, G., Earp, H. S. and Matsushima, G. K. 2007. Macrophages and dendritic cells use different Axl/Mertk/Tyro3 receptors in clearance of apoptotic cells. *Journal of immunology*, **178**: 5635-5642.

68) Shahhosseini, S., Das, D., Qiu, X., Feldmann, H., Jones, S. M. and Suresh, M.

R. 2007. Production and characterization of monoclonal antibodies against different epitopes of Ebola virus antigens. *Journal of virological methods*, **143**: 29-37.

69) Su, E. W., Lin, J. Y. and Kane, L. P. 2008. TIM-1 and TIM-3 proteins in immune regulation. *Cytokine*, **44**: 9-13.

70) Takada, A. 2012. Filovirus tropism: cellular molecules for viral entry. *Front Microbiol*, **3**: 34.

71) Takada, A., Fujioka, K., Tsuiji, M., Morikawa, A., Higashi, N., Ebihara, H., Kobasa, D., Feldmann, H., Irimura, T. and Kawaoka, Y. 2004. Human macrophage C-type lectin specific for galactose and N-acetylgalactosamine promotes filovirus entry. *Journal of virology*, **78**: 2943-2947.

72) Takada, A., Robison, C., Goto, H., Sanchez, A., Murti, K. G., Whitt, M. A. and Kawaoka, Y. 1997. A system for functional analysis of Ebola virus glycoprotein. *Proceedings of the National Academy of Sciences of the United States of America*, **94**: 14764-14769.

73) Takada, A., Watanabe, S., Okazaki, K., Kida, H. and Kawaoka, Y. 2001. Infectivity-enhancing antibodies to Ebola virus glycoprotein. *Journal of virology*, **75**: 2324-2330.

74) Team, W. H. O. E. R. 2014. West African Ebola Epidemic after One Year - Slowing but Not Yet under Control. *The New England journal of medicine*.

75) Towner, J. S., Amman, B. R., Sealy, T. K., Carroll, S. A., Comer, J. A., Kemp, A., Swanepoel, R., Paddock, C. D., Balinandi, S., Khristova, M. L., Formenty, P. B., Albarino, C. G., Miller, D. M., Reed, Z. D., Kayiwa, J. T., Mills, J. N., Cannon, D. L., Greer, P. W., Byaruhanga, E., Farnon, E. C., Atimnedi, P.,

Okware, S., Katongole-Mbidde, E., Downing, R., Tappero, J. W., Zaki, S. R., Ksiazek, T. G., Nichol, S. T. and Rollin, P. E. 2009. Isolation of genetically diverse Marburg viruses from Egyptian fruit bats. *PLoS pathogens*, **5**: e1000536.

76) Ueyama, T., Kusakabe, T., Karasawa, S., Kawasaki, T., Shimizu, A., Son, J., Leto, T. L., Miyawaki, A. and Saito, N. 2008. Sequential binding of cytosolic Phox complex to phagosomes through regulated adaptor proteins: evaluation using the novel monomeric Kusabira-Green System and live imaging of phagocytosis. *Journal of immunology*, **181**: 629-640.

77) Umetsu, S. E., Lee, W. L., McIntire, J. J., Downey, L., Sanjanwala, B., Akbari, O., Berry, G. J., Nagumo, H., Freeman, G. J., Umetsu, D. T. and DeKruyff, R. H. 2005. TIM-1 induces T cell activation and inhibits the development of peripheral tolerance. *Nature immunology*, **6**: 447-454.

78) Valverde, P. 2005. Effects of Gas6 and hydrogen peroxide in Axl ubiquitination and downregulation. *Biochemical and biophysical research communications*, **333**: 180-185.

79) Volchkov, V. E., Feldmann, H., Volchkova, V. A. and Klenk, H. D. 1998. Processing of the Ebola virus glycoprotein by the proprotein convertase furin. *Proceedings of the National Academy of Sciences of the United States of America*, **95**: 5762-5767.

80) Weissenhorn, W., Carfi, A., Lee, K. H., Skehel, J. J. and Wiley, D. C. 1998. Crystal structure of the Ebola virus membrane fusion subunit, GP2, from the envelope glycoprotein ectodomain. *Molecular cell*, **2**: 605-616.

81) Wool-Lewis, R. J. and Bates, P. 1998. Characterization of Ebola virus entry by using pseudotyped viruses: Identification of receptor-deficient cell lines. *Journal*

of virology, **72**: 3155-3160.

82) Wool-Lewis, R. J. and Bates, P. 1999. Endoproteolytic processing of the ebola virus envelope glycoprotein: cleavage is not required for function. *Journal of virology*, **73**: 1419-1426.